Surficial Geology of Flemish Pass:

Assessment of hazards and constraints to development

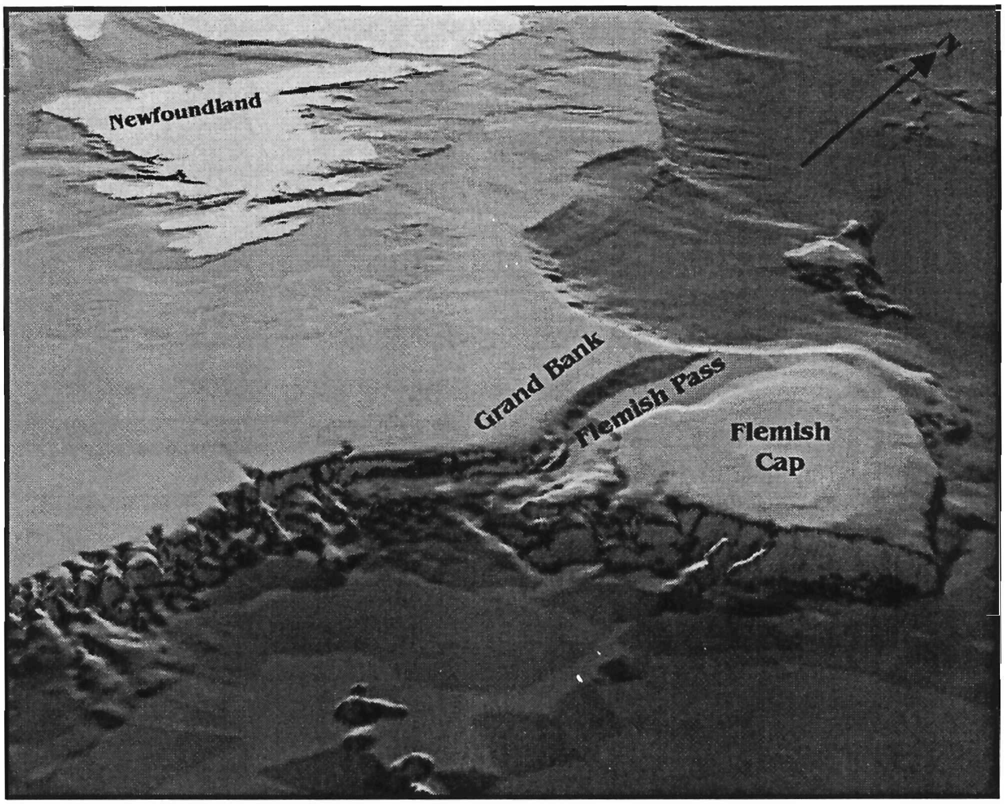

D. Calvin Campbell, David J. W. Piper, Ernest V. Douglas, and Sebastien Migeon

Geological Survey of Canada Open File # 1454

2002

Natural Resources Canada | Ressources naturelles Canada

Canada

GEOLOGICAL SURVEY OF CANADA

OPEN FILE 1454

Surficial Geology of Flemish Pass:
Assessment of hazards and constraints to development

D. Calvin Campbell, David J. W. Piper, Ernest V. Douglas, and Sebastien Migeon

2002

Available from
Geological Survey of Canada
Bedford Institute of Oceanography
1 Challenger Drive
Dartmouth, Nova Scotia B2Y 4A2

Campbell, D.C., Piper, D.J.W., Douglas, E.V., and Migeon, S.
2002: Surficial Geology of Flemish Pass: Assessment of hazards and constraints to development, Geological Survey of Canada, Open File 1454, 61 p.

Open files are products that have not gone through the GSC formal publication process.

TABLE OF CONTENTS

I. Introduction

The Geological Survey of Canada (Atlantic) has conducted research on the surficial geology of Flemish Pass for the past 30 years. Since 1969, seventeen geological expeditions have been conducted in the area. Data collected include regional single beam bathymetry, high resolution seismic reflection profiles, sidescan sonar, as well as a range of sediment samples (piston cores, gravity cores, and box cores). Data collection prior to 1996 concentrated primarily in central Flemish Pass around the Gabriel C-60 and Kyle L-11 exploratory wells. Since 1996, four expeditions provide additional regional information for the northern and southern portions of the Pass.

The purpose of this report is to provide a review of surficial geological hazards and constraints to industrial development in Flemish Pass. The approach will be to revisit the findings presented in previous reports, papers, and articles in light of geological hazards, and to compile and (in some instances) reinterpret the multiple data sets.

Location

Flemish Pass is a mid-slope basin in 1000 metres water depth bounded to the west by the Grand Banks of Newfoundland and to the east by the isolated Flemish Cap. This area covers approximately 30,000 km^2 (Fig. 1a, inset). Four deepwater exploratory wells were drilled during the late 1970's to mid-1980's in Flemish Pass (Fig. 1a). Within the last 5 years, more than 40% of the study area has come under lease by petroleum exploration companies.

Geological Setting

Flemish Pass is a saddle shaped mid-slope basin on the continental slope off the eastern margin of Grand Bank. Its topography allows for the trapping of sediment which elsewhere on the eastern Canadian margin would be transported across the continental slope and rise to the abyssal plain, making it an excellent natural laboratory for the study of upper slope processes (Piper and Pereira, 1992).

Flemish Pass lies above a graben that formed as a result of rifting of the North Atlantic (Grant, 1972). Exploratory wells and regional petroleum industry seismic profiles show that Miocene sediments overly a thick Mesozoic sequence (Kennard et al., 1990). Pliocene and Quaternary sediments have prograded eastwards across a post Miocene unconformity throughout much of Flemish Pass (Piper and Normark, 1989) (Fig. 2A). On the eastern margin of the Pass, these sediments unconformably onlap older sediments on the flanks of Flemish Cap. On the floor of the Pass, Pliocene and Quaternary sediments, for the most part, appear well stratified, interrupted occasionally by large scale amorphous bodies. On the western flank of the Pass, high resolution seismic reflection lines collected along the strike of the Grand Banks slope show complex cut and fill sequences which appear related to depositional lobes observed on the floor of the Pass (Piper and Normark, 1989).

Hazards identified in previous studies

Numerous open file reports and journal articles have been written on the surficial geology of Flemish Pass during the last 20 years. Many of these papers did not focus on geological hazards per se, but most have presented results which have applications for hazard assessment.

Piper and Sparkes (1986) identified 3 distinct periods of sediment failure and debris flow deposition in the upper tens of metres of seabed on the western flank of central Flemish Pass. They recognised similarities between the western margin of Flemish Pass and the upper Scotian Slope west of Verrill Canyon and demonstrated that the Gabriel depositional lobe was fed by a slope gully system developed during the late Pleistocene.

In their discussion, Armstrong et al. (1988) detailed 3 specific implications for hydrocarbon development in Flemish Pass. Unstable hole conditions may be encountered on valley floors on the western flank of Flemish Pass, analagous to the slope channels on the Nova Scotian margin which tend to concentrate boulders. The predominance of silty sediments in Flemish Pass may make the seabed prone to liquefaction. Evidence for shallow gas is widespread in the area, both in the geophysical records and in the sediment samples, and presents a stability risk. Morin and Pereira (1987) conducted infinite slope analysis on cores from the central part of the Pass and concluded that for an average slope of 2.3°, the seabed is stable up to earthquake accelerations of 0.20 g, well above the probable peak acceleration. They too recognised a need to better understand liquefaction potential of the surficial sediments in the area.

II. Data and Methods

High resolution seismic reflection data

More than 4000 line kilometres of seismic reflection data have been collected in Flemish Pass by the Geological Survey of Canada since the late 1960s (Fig. 1b). The seismic source consisted primarily of small (10 to 40 in^3), airgun with a maximum vertical resolution of about 1 m, and Huntec DTS sparker or boomer systems with a maximum vertical resolution of 0.2 m. These data sets were often collected concurrently.

A regional high resolution seismic stratigraphy was developed in earlier reports by Piper and Sparkes (1986), Armstrong et al. (1988), Piper and Normark (1989), Piper and Pereira (1992), and Campbell (1997) for the central part of Flemish Pass. Ties to exploratory wells and radiocarbon dates from piston cores provide age constraints for this stratigraphy. For this study, the stratigraphy has been extended to the north and to the south on the floor of the Pass, as well as onto the western flank of the Pass. The stratigraphy provides a framework for comparison between features seen in the seismic reflection data throughout the Pass.

Initially, a seabed classification scheme, similar to the data presented by Cameron (2000) for the deep water margin off southeast Grand Banks and by Campbell (2000) for the Scotian Slope, using 3.5 kHz echo sounder data was considered. However, the sandy nature of the Flemish Pass seabed results in little sub-bottom penetration using the 3.5 kHz system. Instead, a seabed acoustic facies model was developed using the Huntec

DTS data, resulting in a map of along-track acoustic facies throughout Flemish Pass. The results from this mapping experiment are discussed further below.

Sediment samples

Approximately 70 sediment samples have been collected in Flemish Pass, including box cores, gravity cores, and about 45 piston cores (Fig. 1b). Piston cores have been obtained using the Atlantic Geoscience Centre Long Coring Facility (Moran et al. 1989), except on cruise 96018 when a Benthos corer was used. A 24-m-long core was collected from the N/O Marion Dufresne in 1995 from Sackville Spur using a Calypso corer (Bassinot and Labeyrie 1996). Eighteen of the piston cores were collected during expedition 2001-043 and were not analyzed prior to this report. Core analyses include seabed lithology, sediment grain size, sediment physical properties such as shear strength, plasticity, density, velocity, colour, as well as radiocarbon dates of in situ shells to provide age information. Marsters (1991) presented p-wave acoustic velocity, vane shear strength, water content, bulk density, Atterberg limits, and grain size data from 9 cores collected during the mid 1980's. Campbell (1997) reported on cores collected during expedition 96-018, including eleven cores from Flemish Pass, presenting colour reflectance data from spectrophotometry, Multi-Sensor Track measurements (acoustic velocity, bulk density, and magnetic susceptibility), as well as lithological descriptions. Thirty-one radiocarbon dates are available from cores and are shown in Table 1. Atterberg limits data collected since the report of Marsters (1991) are presented in the Results section.

Cores from Flemish Pass are typically less than 11 m in length, with the exception of MD95-2026. They are used to ground-truth the remotely sensed geophysical data, to characterize the upper 10 metres of seabed, to provide age estimates for the shallowest acoustic reflectors, and to provide sedimentation rates during the late Pleistocene and Holocene.

Deep water sidescan sonar

During the 1980's two separate deepwater sidescan sonar surveys were conducted in Flemish Pass. Over 5000 km^2 of data were collected over the floor and western flank of

Flemish Pass with the Geologic Long Range Inclined Azdic (GLORIA) sidescan sonar system using a 10 to 25 km wide swath width. The GLORIA system has an operational frequency of 6.3-6.7 kHz and, therefore, features up to a few metres sub-bottom will be imaged by this system (Hughes Clarke et al., 1992). Jacobs (1989) previously reported data and interpretation from this survey. Over 750 km^2 of data were collected along the western flank of central Flemish Pass using the SeaMARC I deep towed sidescan sonar system. The system was towed approximately 300 m off the seabed and used a 5 km wide swath. The operational frequency of this system is 27 and 30 kHz, and therefore, there should be little penetration of the subsurface. Pereira et al. (1985) previously reported data and interpretation from this survey.

Surface (and near surface in the case of the GLORIA data set) features recognized on the sidescan sonar imagery were digitized into a geographical information system and compared to features identified in the high-resolution reflection data. In some cases, the sidescan interpretation aided in the interpretation of the sub bottom data, while in other instances, a reinterpretation of the sidescan data, based on recently acquired sub bottom data, has led to new insight.

III. Results

Seismic Analysis

Shallow seismic stratigraphy

Previous studies by Piper and Sparkes (1986), Armstrong (1988), Piper and Normark (1989), Piper and Pereira (1992), and Campbell (1997) have helped to develop and refine a shallow seismic stratigraphy throughout Flemish Pass dating back to the Pliocene. The previous studies were focused on certain geographic areas within the Pass, either because of a lack of data or because of the scope of the study. One of the goals of this study is to compile the seismic stratigraphy of the earlier reports and to expand the seismic interpretation geographically with data collected since 1997.

Table 2 describes the seismic stratigraphy nomenclature used in this report and how it relates to the nomenclature developed in previous reports. Figure 2 illustrates the type sections for the seismic stratigraphy. The type sections were defined on the floor of the central part of Flemish Pass, which is characterized as having continuous, well stratified reflections in the upper few hundred metres below seafloor. There is overlap between the airgun and Huntec stratigraphy, and the green reflector on the Huntec profiles is approximately the green reflector on the airgun profiles. Piper and Normark (1989) recognized several regional horizons on industry multichannel profiles and these provide a framework for the development of the seismic stratigraphy in Flemish Pass (Fig. 2).

General acoustic character

On the airgun profiles, the shallow seismic character (upper 100 metres) of the seabed on the floor of Flemish Pass is predominantly very continuous to discontinuous reflections (Fig. 2). The other common acoustic facies on the floor of the Pass comprises amorphous zones of transparent or chaotic reflections (Fig. 3, 4, 5, and 6). The margins of the amorphous units facies usually have distinct start and end points, either through lateral wedge-shaped pinch-outs into stratified sediment, which is the case in the northern part of Flemish Pass, or as abrupt vertical or subvertical terminations, which is the case near the Gabriel C-60 well. The origin of the amorphous facies is examined further in the discussion section of this report.

On the western margin of the Pass, the airgun profiles show a complex series of unconformities, cut and fill features, and shallow escarpments (Fig. 7). The northwest margin of the Pass has a large (over 75 m of relief) buried escarpment which continues laterally along strike for approximately 45 km. Escarpments of this magnitude have been observed on multibeam imagery on the Scotian Slope in deeper water depths (Pickrill et al., 2001). Sediment waves, or bedforms created by bottom currents are recognizable in some areas of the Pass. In particular, at the foot of the western Flemish Cap slope at about 47° 30' N there is zone of bedforms which have been mapped. The bedforms have a vertical relief of at most a couple metres and wavelengths of about 300 metres (Fig. 8).

Other than adjacent to the type section, it was not possible to extend the seismic stratigraphy on the airgun records below the violet reflector over the floor of the Pass due to a lack of penetration (Fig. 9). On the western flank of the Pass, it was possible to trace the stratigraphy down to the grey reflector (Piper and Sparkes, 1986 and Armstrong et al., 1988). The blue and orange reflectors were traced throughout much of the Pass (Fig. 9). In the Huntec profiles, it was possible to trace reflectors yellow, orange, and red throughout much of the Pass.

As mentioned, a predominant acoustic facies in Flemish Pass are large scale amorphous zones which in the past have been interpreted as debris flow deposits (Piper and Sparkes, 1986) or as sandy depositional lobes (Armstrong et al., 1988). A summary of the stratigraphy of the amorphous zones is shown in Figure 9. The shallowest reflector traced throughout much of Flemish Pass on the Huntec profiles is red (alpha from Piper and Sparkes, 1986). Armstrong et al. (1988) noted that only near the Kyle well has downslope failure or mass movement occurred above this reflector. Data collected elsewhere on the Pass since 1996 agree with this observation. Piper and Pereira (1992) reported that dates from core 87008-013 bracket the red reflector and give it an age between 19.2 ka and 11.8, probably closer to 19 ka, however a re-examination of the data makes this correlation uncertain. In core 87008-015, the red reflector correlates to an interval above a radiocarbon date of 23.6 ka and below Heinrich 2, giving the reflector an age of around 21 ka.

Armstrong et al. (1988) recognised two unconformities near the Kyle well site which were thought to be of local extent and represented the last major period of channel cutting on the Grand Banks slope. Data collected since 1996 has shown that unconformable horizons are widespread through this interval and channel cuts are visible on the floor of the Pass in Huntec data (orange reflector) as well as on the airgun data (the green reflector). To the south, the green reflector is terminated by the shallowest in a series of stacked amorphous bodies (Fig. 9). In the northern part of the Pass (north of the Gabriel well) E. King (personal communication, 2001) recognised a series of stacked amorphous bodies on the airgun data from cruise 99-031 (Fig. 5). The extent of the amorphous zones has been mapped using all the available airgun data and is shown to cover over 2600 square kilometres in plan view and, with the largest body having an average thickness of approximately 50 metres and a volume of 130 cubic kilometres of sediment. The green reflector coincides in the north with the top of the youngest amorphous zone.

The blue reflector (NSRF Green from Campbell, 1997) corresponds to the top of the "d" amorphous zone which comprises part of the Gabriel depositional lobe (Fig. 3). To the south, this reflector corresponds to the top (or approximately the top) of the second amorphous zone in the narrow valley between Hudson's spur and Beothuk Knoll (Fig. 4). In the north, the blue reflector terminates at the margin of the large amorphous zone mentioned earlier.

Acoustic classification of the seabed

Five acoustic facies were identified from the available Huntec data in Flemish Pass (Fig. 10). The facies types represent the range from continuous parallel reflections with up to 50 msec (twtt) of penetration to incoherent sub-bottom with little penetration of the seafloor. The acoustic facies were defined as:

Facies Type A: Parallel to sub-parallel continuous reflections

Facies Type B: Parallel, but discontinuous reflections.

Facies Type C: Parallel reflections with abundant acoustic masking and bright spots.

Facies Type D: Hummocky seabed with transparent sub-surface. Occasionally surface shows parallel reflections before becoming transparent.

Facies Type E: Sub-surface has incoherent or prolonged strong reflections.

A map showing the along track acoustic classification of the seabed is shown in Figure 11. The shallow subsurface character of Flemish Pass is predominantly parallel continuous to discontinuous reflections (Facies A and B). In areas of shallow depositional lobes, the acoustic facies is typically parallel reflections with abundant acoustic masking to hummocky seabed with transparent subsurface (Facies C and D). On steep slopes and in areas shallower than ~500 metres, the seabed acoustic properties produce incoherent or prolonged strong reflectors on the Huntec DTS profiles (Facies E).

Sediment Samples

Sedimentology

Over 70 sediment samples have been collected in Flemish Pass, including 18 piston cores during expedition 2001-043. Of the 27 piston cores processed, 14 were re-examined and are summarised in Figures 12 and 13. A transect of six cores were examined in greater detail and are presented in Figure 13. Locations of cores are shown in Figure 1b. The piston cores are typically 5 to 10 m in length and consist of mud to sandy mud with thick sandy and silty intervals (Piper and Pereira, 1992, Morin and Pereira, 1987).

In Figure 12, the cores have been classified based on colour changes and visual estimates of texture. The cores have been sub-divided into units of mud, which is predominantly clay and silt; sandy mud, which is mud with noticeable sand grains; sand, which here is typically clean sand with little or no clay or silt; and silt. The narrow column adjacent to each lithologic column illustrates the downcore location of Heinrich (H) ice-rafting layers (Heinrich, 1988; Piper and Skene, 1998) and estimates of the last glacial maximum (LGM) interval which is based on the presence of distinctive purplish-red sediment often found between H1 and H2 (Piper and deWolfe, 2002).

Piper and Pereira (1992) identified four broad mechanisms for sedimentation in Flemish Pass based on cores:

Turbidity currents: turbidites identified on the basis of characteristic sedimentary structures such as graded sand beds, laminated muds, and poorly sorted sand beds exhibiting variable grading.

Debris flows: debrites identified on the basis of mud clasts and stones in a muddy matrix with variable internal structure and a sharp base.

Hemipelagic sedimentation: a broad category which is less confidently characterised because of a lack of distinctive features. It ranges from grey mud with scattered stones to winnowed gravely sandy mud.

Detrital carbonate rich ice rafting events: Morin and Pereira (1987) recognised a beige brown carbonate rich layer which was correlable between several cores in southwest Flemish Pass. Similar layers have been reported by Piper and Skene (1998) (their detrital carbonate layers) and by Campbell (1997) as Heinrich layers (Heinrich, 1988). Spectrophotometry data on cores from Flemish Pass allows for the identification of Heinrich layers as noticeable increases in the L* (black to white, Adobe, 2002) colour value (Fig. 14)

Lithostratigraphy

The stratigraphic section revealed by piston coring varies according to physiographic setting. On the western slopes of Flemish Pass, the stratigraphic section is represented by core 85044-03 (Fig. 12). This consists principally of muds with some coarse-grained ice-rafted detritus, with at least 6 horizons rich in detrital carbonate. Interbedded sandy turbidites are most abundant between 2 and 3.5 metres below seafloor (mbsf).

On the floor of the central part of Flemish Pass, cores such as 77014-08 and 91020-079 (Fig. 12) penetrate a succession of silty muds with ice-rafted detritus, thin sand and mud turbidites, and two horizons rich in detrital carbonate before either stopping at or penetrating thick bedded sand turbidites. On the eastern margin of Flemish Pass, thick mud turbidites are sampled in core 87008-013 (Fig.12).

On the eastern slopes of Flemish Pass, in cores such as 96018-06 (Fig. 12 and 13), sediment consists principally of mud with sparse ice-rafted detritus. A few sand beds with gradational boundaries are interpreted as contourites (cf. criteria in Nelson et al. 1993). Several horizons rich in Heinrich detrital carbonate are present.

On Sackville Spur, core MD95-2026 (Fig.15) penetrated 8 m of sandy gravelly mud, overlying 4.5 m of grey mud and then a further 12 m of gravelly sandy mud. Some horizons rich in detrital carbonate occur throughout the core.

Significance of Heinrich layers

In the Labrador Sea and on the Newfoundland margin, episodic beds of detrital carbonate have been recognised and correlated with Heinrich events, times of rapid iceberg calving from Hudson Strait and other glacial icesheet outlets (Andrews and Tedesco 1992). These detrital carbonate beds are commonly termed Heinrich layers and those associated with the last (Wisconsinan) glaciation have been numbered from 1 to 6. The ages of Heinrich layers are well known from radiocarbon and other dating studies (e.g. Bond and Lotti 1995), so that once a particular Heinrich layer is identified, for example by radiocarbon dating, under- and overlying Heinrich layers can be used to provide a chronology for the sediment sequence. The distribution of Heinrich layers H1 and H2 in Flemish Pass, with a characteristic intervening purplish mud with ice-rafted detritus, was documented by Piper and Skene (1998). The sequence of Heinrich layers back to H4 has been determined in core 96018-006 by radiocarbon dating (Rashid et al., 2002), with H3 and H4 having a lower detrital carbonate content than H1 and H2. In core MD95-2026, the 52.5 ka radiocarbon date allows recognition of the underlying H6 and overlying H5 or H5a Heinrich layers and tentative identification of shallower Heinrich layers, with H1, H2 and H3 identified with confidence. This succession can be tentatively correlated with cores 85044-003 and 99031-004 (fig. 13).

Physical Properties

Physical property data on cores from Flemish Pass can be found in reports by Morin and Pereira (1987), Marsters (1991), Christian et al. (1991), and Campbell (1997) and include index property measurements, undrained shear strength, Atterberg limits, colour reflectance, as well as limited data from consolidation testing.

Atterberg limits tests were conducted on particularly clayey or silty clayey intervals. Recent measurements on cores collected during 1996 and 1999 (Fig. 16) agree with the results from Marsters (1991, her Figure 2) and show that most of the samples can be classified using the Unified Soil Classification scheme as inorganic clays of low to medium plasticity. Undrained shear strength measurements by Marsters (1991) show values which typically range from 4 to 10 kPa with occasional measurements of more than 25 kPa. Christian et al. (1991) also showed shear strengths in this range. These measurements appear low compared to recent analysis of cores from the Scotian Slope. Undrained shear strength measurements from cores collected in 2001 will verify whether or not the shear strength of sediments from Flemish Pass are significantly lower than sediments from the Scotian Slope.

Chronology

Thirty-one radiocarbon dates are available from Flemish Pass. These data show that the piston cores sample back to at least 40 ka. Figure 17 shows late Pleistocene sedimentation rate on the floor of Flemish Pass, based on radiocarbon dates, of about 37 cm/ka. Sedimentation rates vary greatly through time and space in Flemish Pass. For example, core 87008-13 (Fig. 12) shows a late Pleistocene sedimentation rate of about 70 cm/ka, whereas most cores show a Holocene rate of about 5 cm/ka . The data from the flanks of the Pass show much more variability in rate and are generally lower than the data from the floor of the Pass. An average sedimentation rate of 25 cm/ka was used for age estimation of features beyond the penetration of piston cores.

Sidescan sonar

Data and results from the two deepwater sidescan surveys in Flemish Pass were reported on by Pereira et al. (1985) (SeaMARC I) and Jacobs (1989) (GLORIA).

The SeaMARC I survey (CCGS Hudson cruise 84-035) was run on the western flank of central Flemish Pass. The survey track paralleled slope along the 1100 m isobath and then turned westward up the slope near the Gabriel C-60 well. The sidescan images show that most of the seabed surveyed has little relief. There are discernable downslope trending lineations, areas of undulating seabed relief, and linear and curvilinear features. Pereira at al. (1985) interpreted several features from the sidescan records including hummocky relief on depositional mounds, escarpments with < 10 m relief, escarpments with 10-30 m relief, escarpments with > 30 m relief, a moat around a local high, small sediment mounds and hills (diapirs), as well as two populations of iceberg scours on the upper slope.

The GLORIA surveys (RRS Discovery cruise 111 and a short line collected during MV Farnella cruise 2/81) covered a much wider swath than the SeaMARC survey, with coverage over much of the floor of the Pass and a portion of Sackville Spur. Again, the GLORIA data shows that the floor of the Pass has very little relief. There are areas of high acoustic backscatter, acoustic shadows, and elongate lobes. Jacobs (1989) used the GLORIA records and accompanying sub-bottom data to interpret current erosional features in the south, depositional lobes at the foot of the western margin of Flemish Pass with elongate diapirs marking the edges of lobes, large areas of high acoustic backscatter interpreted as failure triggered turbidity current deposits, and possible downslope sediment movement on the southern flank of Sackville Spur.

IV. Synthesis of near seabed geology

A map which summarizes the near seabed geology in Flemish Pass was produced from the examination of the existing sub-bottom profiles, sidescan sonar mosaics, and sediment cores (Fig. 18). Clearly a map of this scale cannot identify every feature within the study area, but it does demonstrate the regional distribution of the near seabed geology. It should be mentioned that the accuracy of the extent of some features is governed by the data coverage.

Major amorphous zones

In many areas of Flemish Pass, it is possible to recognise incoherent or transparent zones in the seismic reflection and Huntec DTS data. The map shows areas where these zones are particularly severe and exceed a vertical thickness of 10 metres (Fig. 18).

Previous studies have attempted to determine the origin of the amorphous zones, in particular the Gabriel lobe, a mounded feature near the Gabriel C-60 well. This large amorphous zone was originally described as a debris flow or slump deposit by Geomarine (1979) in a well site survey. Pereira et al. (1985) concluded that the lobe was a mass flow deposit overlain by turbidites based on the hummocky surface relief and transparent character of the sub surface. Piper and Sparkes (1986) interpreted the lobe as a failure deposit, explaining the abrupt termination of the margins of the homogenous body as indicative of in situ failure due to rotational slumping. Armstrong et al. (1988) suggested that the acoustically amorphous zones were not a result of mass failure, but were due to shallow gas dispersed in more permeable sediments. This idea was based on the observation of gas in sediment cores collected near the lobe, that sandier intervals in cores collected adjacent to the lobe corresponded to more amorphous zones in the lobe, and that major reflectors can be seen to be continuous into some of the amorphous zones. Piper and Pereira (1992) referred to it as a depositional lobe. Examination of data collected since 1996 shows the presence of large amorphous zones in the northern and southern extents of the floor of the Pass not previously reported (Fig. 18).

The zones have geometries ranging from predominantly depression filling, with a convex upper surface, abrupt subvertical lateral margins and a thinning basinward margin, to predominantly depression filling with a flat or concave upper surface and thinning towards the margins. The upper surface can appear hummocky in relief. Some have a lenticular appearance, for example the shallow amorphous zone to the right on Figure 8. In most cases, these zones are associated with headwall escarpments or down slope trending channels. Given the above criteria, the amorphous zones are interpreted as mass transport deposits, which may include translational and rotational slides, debris flows and turbidity current deposits. They vary greatly in size and extent, with some appearing to be very localized while others are regional, for example the shallowest mass transport deposit on the flanks of Sackville Spur has been delineated using several airgun profiles and represents approximately 130 cubic kilometres of failed sediment.

Age and origin of mass transport deposits

The age of the youngest failure and debris flow in the southern part of Flemish Pass is determined to lie between the LGM and H2 in core 96018-12 (Fig. 19) and in core 85044-03 (Fig. 20, also Figure 10 in Piper and Pereira, 1992). At the lobe near the Gabriel C-60 well, the location and style of the debris-flow deposits suggests that they may result from confined flow of debris down the slope channel. The shallowest major debris-flow deposit (a) is dated by seismic correlation (Fig. 21 and 22) to the younger part of MIS 5. Deposit (b), a little above green, corresponds to the younger part of MIS 7. Further extrapolation assuming constant sedimentation rates is not constrained by recognition of acoustic facies, but suggests that deposit (c) formed in MIS 9. Further linear extrapolation of sedimentation rates would imply an age of about 0.9 Ma for the violet reflector. Piper and Normark (1989) inferred that shelf-crossing glaciation first took place at about the violet reflector, on the basis of the seismic architecture of the continental slope. The age of the violet reflector thus suggests a correlation with the major glaciation in MIS 22.

The age of the uppermost deeply buried failure on the flanks of Sackville Spur can be estimated by extrapolation of sedimentation rates in MD95-2026. This core shows rather similar sedimentation rates both in glacial (MIS 2-4) and interglacial (MIS 5) conditions, as also noted for Orphan Knoll (Piper and Toews, in press), of approximately 0.1 m/kyr. Extrapolation of such sedimentation rates to the thickness of undisturbed sediment on Sackville Spur above the violet reflector is consistent with the age estimate near the Gabriel C-60 well, but such an estimate has a very large associated error. The presence of two deeply buried and one near-surface debris-flow deposit above the violet reflector in northern Flemish Pass suggests a mean recurrence interval of 0.3 Ma.

Distribution and age of major debris-flow deposits provides some constraints on their origin. Large failures may be triggered by large earthquakes (greater than magnitude 6). The historical record of seismicity around the Grand Banks is poorly known, but rare large earthquakes similar to the 1929 Grand Banks earthquake are to be expected on the passive margins, probably concentrated along old basement lineaments (Keen et al., 1990), with recurrence intervals probably in the range of 100 ka (Piper and Normark, 1982).

Failures may also be triggered by high pore pressures, which may be induced by seismic accelerations or by melting of gas hydrates as a result of reduction in pressure due to falling sea level or increase in temperature due to warming of bottom waters (e.g., Kayen and Lee, 1991). A bottom-simulating reflector indicating the presence of gas hydrates has been recognised from industry seismic lines beneath the topographically complex Sackville Spur (Thurber Consultants Ltd. 1985) and suggests that gas hydrates may be present elsewhere in Flemish Pass which is within the pressure-temperature threshold for hydrate formation. Free gas migrating up from the base of the hydrate layer may be responsible for acoustic wipeouts seen locally in high-resolution seismic data (Armstrong et al. 1989). Bottom water temperature in Flemish Pass is buffered by the supply of cold arctic water through the Labrador Current, so that times of gas hydrate melting are likely restricted to periods of falling sea level between interglacial and glacial maximum conditions.

Sediment failure may also result from progressive deformation or weakening of slip planes such as faults or weak horizons above which creep has taken place. This type of failure is common in areas where slopes are steepened by active tectonism or salt deformation. Such slope steepening is not occurring in Flemish Pass. Such failures may also result from rapid sediment loading or perhaps loading by ice. Failures resulting from progressive deformation rather than a triggering mechanism are unlikely to occur simultaneously in different areas, unless due to a widespread loading process. Simultaneous failure on both flanks of Flemish Pass to create the widespread debris-flow deposits on the floor of Flemish Pass suggests that progressive deformation can be excluded as in initiation process. Failure headscarps are in quite deep water, well away from any shelf edge ice or sediment loading. Triggering by a large earthquake appears most likely. The tentative chronology implies that failure is not related to glacial and glacio-eustatic sea-level cycles, suggesting that destabilisation by gas hydrate melting is unlikely.

The three youngest small debris-flow deposits on the Gabriel lobe, (a), (b) and (c) (Fig. 21), all seem to have occurred during interglacial conditions (Fig. 22) (see discussion in section V). It is unclear whether this represents a pattern related to cause. In general during the late stages of interglacials, there was a progressive fall in sea level as icecaps grew towards glacial conditions. The youngest debris-flow deposit in southern Flemish Pass (Fig. 19) also occurred during falling sea level, from MIS stage 3 to the Last Glacial Maximum. Falling sea level results in less hydrostatic pressure in seabed sediments and hence a melting of gas hydrate. Falling sea level also results in increased cyclic wave loading of outer shelf edge deposits. The observed pattern of younger debris-flow deposits in the central part of Flemish Pass may thus indicate a role for gas hydrates and/or cyclic loading in triggering failure.

Sediment wave field

Huntec and airgun data from cruises 96-018 and 99-031 show distinct undulating bedforms (Fig. 8) with internal reflections typical of migrating sediment waves. These bedforms migrated up current, similar to the sediment waves discussed in Migeon et al. (2001). Sand beds and clayey sand beds in cores from this area have been interpreted as probable contourites. On the Huntec data they appear to be at or near the seabed, however, cores show that they do not appear to be currently active.

Sand sheet

Jacobs (1989) recognised an area of high acoustic backscatter on the GLORIA data. Huntec data from this area shows distinct shallow, thin, acoustically-incoherent lenses which are similar to the sand lenses on Hueneme Fan reported by Piper et al. (1999) (Fig. 23). The lobe shaped plan view geometry of the sand sheet (Fig. 18) and the fact that it is immediately basinward from the Gabriel lobe suggest that it consists of proximal turbidites. Three cores from this area show evidence of thick sand. Core 91020-079 penetrated only 2 metres before stopping in sand (Fig. 12, 13). Cores 96018-008 and 77014-008 cored through several metres of sand and clayey sand at about 4 metres below the surface (Fig. 12,13). The acoustic evidence combined with observations from cores indicate a high probability of widespread, metres-thick sand bodies in the shallow subsurface east of the Gabriel lobe.

Shallow diapirism

Headspace gas

Shallow diapirism has been identified around the Gabriel lobe (Armstrong et al., 1988 and Jacobs, 1989) (Fig. 3 and 18). The features have been reported to have a gaseous composition based on the gassy nature of cores from the area and the acoustic masking seen in subbottom profiles. At the Gabriel lobe, the diapirs probably are formed through the upward hydraulic movement of fluids that are trapped within rapidly deposited sediments. Fluids and gas would migrate readily in this area because of the abundance of sand and silt.

New data collected during 1999 and 2001 show the presence of severe shallow diapirism on the crest of Sackville Spur. The features are very impressive in Huntec profiles (Fig. 24) and are similar to the pagoda structures described by Emery (1974). The diapirs appear as stratified mounds with acoustically masked interiors and have a vertical relief of up to 10 m. Because these features are not near a major depositional lobe, the fluids required to produce them must be from a different source. Gas hydrates are thought to exist in the Sackville Spur area based on the identification of a Bottom Simulating Reflector (BSR) in industry seismic data (Thurber Consultants Ltd., 1985). A BSR is formed at the base of the gas hydrate stability field and mimics the seabed because the stability field changes with overlying pressure. Therefore, these diapirs might be formed by the updip migration of fluids and gas to the crest of Sackville Spur.

V. Seismic Stratigraphy from Huntec DTS Profiles on the floor of Flemish Pass

High-resolution Huntec sparker profiles from the floor of Flemish Pass show several distinct acoustic facies (Fig. 23) that can be correlated with cores and can be traced into debris-flow deposits in the lobe-like feature near the Gabriel C-60 well (Figs. 3, 21). In the upper 2 m of Holocene and upper Pleistocene sediment, reflections are parallel and of relatively high amplitude. Locally, small irregularities (Fig. 23, inset) may represent incipient sediment waves. This is recognised as acoustic facies I. There is a similar development of uniform thickness between the orange and yellow reflections, although small irregularities are restricted to the interval immediately above yellow. Around the red reflector, the interval corresponding to thick sands in cores shows 1-2 m-thick, acoustically incoherent beds, interpreted as massive sand by correlation with acoustic facies V of Piper et al. (1999). These incoherent units pass laterally into parallel reflections (Fig. 23 inset). Some reflections are of high amplitude. This is termed acoustic facies II. A similar facies showing high amplitude reflections and lateral pinchouts is also present immediately below the yellow reflector. Acoustic facies III also shows progressive thinning towards the edge of Flemish Pass, although clear onlap is not visible. Reflections tend to be of lower amplitude than in facies I and II. The development of acoustic facies III above the green reflector pinches out towards the lobe near the Gabriel C-60 well and is overlain by a debris-flow deposit (Figs. 23, 21). Acoustic facies IV is similar to acoustic facies III in showing some thinning against topographic features, but also shows some draping over the irregular top of debris-flow deposits.

The section on the floor of Flemish Pass can be dated using both core stratigraphy and the correlation of the orange seismic marker with the MIS 4/5 boundary (Fig. 22). Core MD95-2026 on Sackville Spur shows approximately constant sedimentation rates in glacial and interglacial conditions. If this uniformity in sedimentation rates can also be applied to the floor of the Pass, then the estimate age of the yellow reflector would be 110 ka. Cores from the floor of Flemish Pass show a lower Holocene than glacial sedimentation rate, suggesting that the age of the yellow reflection is underestimated. The yellow reflection marks a transition from acoustic facies I to II, analogous to that between the Holocene and late glacial (Fig. 23). Thus a correlation of the yellow reflector with the MIS 6 to 5 transition at about 127 ka seems reasonable. Extrapolation of this interpretation places the green reflector, with its overlying development of acoustic facies I (Fig. 23), at about 230 ka, probably marking the top of MIS 8 (Fig. 22).

The stratigraphic section on the floor of Flemish Pass can be correlated into the area of sediment waves on the northeastern edge of Flemish Pass (Fig. 8). The uppermost 2-4 m of the seismic-reflection profile shows short-wavelength irregularities, similar to those on the floor of Flemish Pass, that overlie prominently migrating sediment waves, 5-15 m thick, with wavelengths of 0.7 - 1.5 km. At about the orange reflection, there is an abrupt change to waves with a longer wavelength and a more aggradational architecture. The long-wavelength features above and below the orange reflector closely resemble muddy sediment waves described in the literature (e.g., Migeon et al. 2001), built of mud or of mud with thin silt and sand beds. The short-wavelength features at the seabed may be sandy bedforms, similar to those imaged in the Gulf of Cadiz (e.g. Nelson et al. 1993), whose presence is suggested by sand beds up to 50 cm thick in some cores from the eastern flank of Flemish Pass.

Near the Gabriel C-60 well, the stratigraphic section on the floor of Flemish Pass can be linked to the stratigraphy of the acoustically amorphous units that build the lobe. At least six stacked amorphous units, termed (a) to (f), are recognised (Figs. 3, 21). The shallowest prominent acoustically-amorphous unit (a) pinches out just below the orange reflector. Based on the chronology developed above, this would correspond to the top of MIS 5. Two deeper horizons of acoustically amorphous units are recognised in Huntec seismic data: unit (b) a little above the green reflector and unit (c) a little above the blue reflector (Fig. 21). In airgun seismic profiles (Fig. 3), units (d) and (e) are comparable in character to (a), (b) and (c), whereas unit (f) is much thicker and resembles the thick debris flows in the northern part of Flemish Pass (Fig. 5). Unit (f) overlies the violet reflector and appears to be at the same stratigraphic level as the deeper debris-flow deposit in Figure 3.

VI. Interpretation of glacial history through the last glacial cycle

Core to seismic correlation suggests that several facies associations can be recognised in Flemish Pass.

(i) The Holocene is represented by condensed sedimentation and very silty winnowed sediment (Piper et al. 1991). In MD95-2026, it has a high sand and gravel content.

(ii) The interval from H0 to a little below H2 generally has Heinrich layers interbedded with ice-rafted gravelly muds and thin turbidite sands. (Core 87008-13 on the eastern side of Flemish Pass is unusual in having thick mud turbidites). Some deposits on lobes near the Kyle L-11 and Gabriel C-60 wells were interpreted as debris-flow deposits by Piper and Pereira (1992). In the sediment-wave field, this interval is correlated with the development of sediment waves (Fig. 8). Piper and Pereira (1992) inferred that much of the sediment was derived from proglacial plumes originating on the Grand Banks of Newfoundland.

(iii) From a little below H2 to just above H3, many cores on the west side of Flemish Pass have abundant sandy turbidites. On the floor of Flemish Pass, these sands are commonly too thick to penetrate with the piston corer (Fig. 15). Sands onlap relief on the floor of Flemish Pass (Fig. 22). On the western flank of Flemish Pass, this interval is marked locally by an erosional unconformity (red reflector, alpha of Piper and Pereira 1992). At this time (ca. 25 ka), global sea levels had not yet fallen to the Last Glacial Maximum lowstand. We interpret the abundant sands as evidence of a major supply of coarse sediment to the upper slope, presumably from a wet ice margin. In the sediment-wave field, this interval is also correlated with the development of sediment waves.

(iv) An interval that extends from just above H3 to below H6 is rather similar to the interval (ii), with muds and thin turbidites on the western margin of Flemish Pass. It corresponds to acoustic facies III on the floor of Flemish Pass (Fig. 22) and to progradational sediment waves in the sediment-wave field (Fig. 8).

(v) below H6, corresponding approximately to the orange reflector, cores on the western side of Flemish Pass sample the top of a distinctive chocolate-coloured mud of uncertain origin, that corresponds to a 4 m-thick transparent interval in Huntec DTS profiles (Fig. 20). In the sediment-wave field (Fig. 8), this interval is correlated with the more aggradational sediment waves below the orange reflector. This unit dates from MIS 5. At the lobe near the Gabriel C-60 well, debris-flow unit A pinches out into this succession, a short distance below the orange reflector.

(vi) At the base of this mud interval, in core MD95-2026, a very sandy interval with light oxygen isotopes (Fig. 15) resembles Holocene sediment and corresponds to MIS 5e, the peak of the Sangamonian interglacial. Short-wavelength features possibly representing sandy sediment waves are seen on the floor of Flemish Pass at this stratigraphic level (just above the yellow reflector in Figure 22).

(vii) The deeper section below the last interglacial is sampled only in MD95-2026 and has sediment similar to intervals (ii) and (iv).

VII. Geohazards and constraints to hydrocarbon development

The assessment of shallow geohazards in deep-water hydrocarbon basins evolves in complexity as development progresses from exploration to production. At the exploration stage, emphasis is on the identification of potential geohazards and their impact on drilling. In contrast, if production is to take place, a more sophisticated analysis of risk is required. This includes the identification of potential geohazards over the lifetime of the field, the assessment of recurrence interval of natural geohazards, and the development of a geological model for the upper few hundred metres of sediment, which will guide the location of expensive geotechnical boreholes. The geological model together with 3-D high-resolution seismic analysis allows geotechnical properties to be extrapolated from boreholes over the entire area of concern. Engineering modelling can then provide estimates of the factor of safety for slope instability under various scenarios of both natural triggers such as seismicity and induced triggers such as increase in pore pressure due to well control problems or seabed loading by production facilities.

In Flemish Pass, the four deep-water wells drilled in the 1980's and the well-site surveys provided considerable experience with drilling conditions and shallow geohazards. Shallow gas is present in Flemish Pass, but did not result in significant well control problems. No problems with boulder beds were reported, although the potential for boulder concentrations exists both in slope channels and in areas of interglacial winnowing by the Labrador Current. No wells were drilled in areas on the floor of Flemish Pass where there is a hazard of thick loose sand beds. These beds are of limited geographic extent northeast of the Gabriel well and correlate with an inferred glacial advance at about 25 ka. During earlier glaciations in MIS 6, 8, 10 and 12 and perhaps earlier, similar thick sand beds are likely on the floor of Flemish Pass.

The synthesis of Quaternary geology reported here provides some of the background information required for quantitative risk assessment for production. First, it provides quantitative estimates of recurrence of some triggering mechanisms for slope instability. The recurrence interval of earthquakes large enough to trigger regional failures appears very low, approximately 0.4×10^6 years. Natural triggering of failures near the edge of the Grand Banks, perhaps by melting of gas hydrates, also has a low recurrence interval (1.0×10^5 years near the Gabriel C-60 well). Cores do show common turbidite deposits during Heinrich events: their origin is unknown but may be related to the very high rates of sediment deposition during Heinrich events and the likely abundance of iceberg scour impacts destabilising surficial sediment on the slope. Natural risk of sediment failure thus appears very low and can be quantified.

We have presented a geological model that relates variation in sediment types in different parts of Flemish Pass to variation in conditions during glacial cycles. This model can be extrapolated to several hundred metres sub-bottom, to the violet reflector representing the oldest shelf-crossing glaciation. We are currently measuring geotechnical properties in a suite of piston cores collected in August 2001 that will provide some information on the variation in shear strength and other geomechanical properties within Flemish Pass. Older data have been reported by Morin and Pereira (1987) and Marsters (1991). Observations of diapirism above debris-flow deposits (Piper and Pereira 1992) indicates that the deeper debris flows deposits, beyond the reach of piston cores, are underconsolidated and thus have the potential to act as weak beds during continuous deformation. The lack of typical creep folds in Flemish Pass suggests that continuous deformation is likely unimportant. Analogy with the Scotian Slope (Pickrill et al. 2001) suggests that such creep deformation may occur upslope from highly eroded slopes, such as are found on the northern slope off Flemish Pass and Sackville Spur, where weak deeply-buried layers outcrop downslope. The geological model also provides a framework for planning future geotechnical boreholes to provide deeper regional geotechnical assessment. The risk of sediment failure in Flemish Pass would be highest for triggers directly related to hydrocarbon development and quantitative slope stability analysis will be required to assess these hazards and risks.

VIII. Acknowledgements

We thank Gary Sonnichsen and Ned King for sharing of data and Jon Mackie and Ann Miller for discussions. Work was funded by the Canada Program for Energy R&D (PERD), project 532211. Acquisition of core MD95-2026 was funded by the Geological Survey of Canada and NSERC through the CSHD project and the isotopes reported by Mudie et al. (1997) were determined by Dr A.E. Aksu, Memorial University of Newfoundland. Studies of sediment failure and gas hydrates are supported by the NSERC-funded Can-COSTA project.

IX. References

Adobe, 2002. Technical guides - Color Models, CIELAB. http://www.adobe.com/support/techguides/color/colormodels/cielab.html . Date accessed: 15 July 2002.

Andrews, J.T. and Tedesco, K., 1992, Detrital carbonate-rich sediments, northwestern Labrador Sea: implications for ice-sheet dynamics and iceberg rafting (Heinrich) events in the north Atlantic: Geology, v. 20, p. 1087-1090.

Armstrong, R., Piper, D.J.W., and Pereira, C.G.P. 1988. Pleistocene stratigraphy and sedimentation of western Flemish Pass: a seismostratigraphic interpretation. Geological Survey of Canada, Open file 1741.

Bassinot, F. and Labeyrie, L. 1996. Images MD 101. Rapport NO 96-1, IFRTP, 217 p.

Bond, G.C. and Lotti, R., 1995. Iceberg discharges into the North Atlantic on millenial time scales during the last glaciation. Science, v. 267, p. 1005-1010.

Cameron, G.D. 2000. Acoustic evidence for shallow gas and seabed classification along selected ship tracks on the deep-water margin of the Grand Banks of Newfoundland. Geological Survey of Canada, Open File 3762.

Campbell, D.C. 1997. Report on data from cruise Parizeau 96-018 to Flemish Pass. Geological Survey of Canada (Atlantic) internal report.

Campbell, D.C. 2000. 3.5 kHz sub-bottom profiler seabed classification along selected ship's tracks on the Scotian Slope. Geological Survey of Canada, Open File 3928.

Christian, H.A., Piper, D.J.W., and Armstrong, R. 1991. Strength and consolidation properties of surficial sediments, Flemish Pass: effects of biological procesess. Deep-Sea Research, 38: 663-676.

Emery, K.O. 1974. Pagoda structures in marine sediments. Gases in marine sediments, ed. I.R. Kaplan, Plenum Press, New York, 309-317.

Geomarine Ltd. 1979. Wellsite survey Esso Voyageur Gabriel C-60, Flemish Pass. Report to Esso Canada Resources Ltd., Halifax, N.S.

Grant, A.C. 1972. The continental margin off Labrador and eastern Newfoundland: morphology and geology. Canadian Journal of Earth Sciences, 9: 1394-1430.

Heinrich, H. 1988. Origin and consequences of cyclic ice rafting in the northeast Atlantic Ocean during the last 130,000 years. Quaternary Research, 29: 142-152.

Hughes Clarke, J.E., O'Leary, D. and Piper, D.J.W. 1992. The relative importance of mass wasting and deep boundary current activity on the continental rise off western Nova Scotia. Geologic evolution of Atlantic continental rises, ed. C.W. Poag and P.C. de Graciansky, van Nostrand Reinhold, New York, 266-281.

Jacobs, C.L. 1989. Sedimentary processes along Flemish Pass, offshore eastern Canada: a GLORIA and high-resolution seismic reconnaissance. Canadian Journal of Earth Sciences, 26: 2177-2185.

Kayen, R.E. and Lee, H.J., 1991, Pleistocene slope instability in gas hydrate-laden sediment on the Beaufort Sea margin: Marine Geotechnology, v. 10, p. 125-141.

Keen, M.J., Adams, J., Moran, K., Piper, D.J.W., and Reid, I., 1990. Earthquakes and seismicity. in M.J. Keen and G.L. Williams, eds., Geology of the continental margin off eastern Canada, Geology of Canada, no. 2: Geological Survey of Canada, pp. 793-798.

Kennard, L., Schafer, C., and Carter, L. 1990. Late Cenozoic evolution of Sackville Spur: a sediment drift on the Newfoundland continental slope. Canadian Journal of Earth Sciences, 28: 863-878.

Marsters, J.C. 1991. Physical properties of sediments from Flemish Pass. Geological Survey of Canada, Open File 2421.

McIntyre, A., Ruddiman, W.F., Karlin, K. and Mix, A.C., 1989, Surface water response of the Equatorial Atlantic Ocean to orbital forcing: Paleoceanography, v. 4, p. 19-55. [see also SPECMAP Archive #1. IGBP PAGES/World Data Center-A for Paleoclimatology Data Contribution Series # 93-031. NOAA/NGDC Paleoclimatology Program, Boulder CO, USA].

Migeon, S., Savoye, B., Zanella, E., Mulder, T., Faugères, J.-C., and Weber, O. 2001. Detailed seismic-reflection and sedimentary study of turbidite sediment waves on the Var Sedimentary Ridge (SE France): significance for sediment transport and deposition and for the mechanisms of sediment-wave construction. Marine and Petroleum Geology, 18: 179-208.

Moran, K., Piper, D.J.W., Mayer, L.A., Courtney, R., Driscoll, A.H. and Hall, R., 1989, Scientific results of Long Coring on the eastern Canadian continental margin: Offshore Technology Conference, 1989, OTC paper 5963, p. 65-71.

Morin, P., and Pereira, C.G.P. 1987. Sedimentology, geotechnical properties and stability anlysis on the continental slope, east of the Grand Banks of Newfoundland. Marine Geotechnology, 7: 289-316.

Mudie, P.J., Piper, D.J.W., and Aksu, A.E., 1997, Quaternary ice-rafting and ice-margin events around the Grand Banks of Newfoundland, NW Atlantic, 40-50 N: EOS, Transactions AGU, v. 78, p. F28.

Myers, R.A. and Piper, D.J.W., 1988, Seismic stratigraphy of late Cenozoic sediments in the northern Labrador Sea: a history of bottom circulation and glaciation: Canadian Journal of Earth Sciences, v. 25, p. 2059-2074.

Nelson, C.H., Baraza, J. and Maldonado, A., 1993, Mediterranean undercurrent sandy contourites, Gulf of Cadiz, Spain: Sedimentary Geology, v. 82, p. 103-131.

Pereira, C.P.G., Piper, D.J.W., and Shor, A.N. 1985. SeaMARC I midrange sidescan sonar survey of Flemish Pass, east of the Grand Banks of Newfoundland. Geological Survey of Canada, Open File 1161.

Pickrill, R., Piper, D.J.W, Collins, J.T., Kleiner, A., and Gee,L. 2001. Scotian Slope mapping project: the benefits of an integrated regional high-resolution multibeam survey. Offshore Technology Conference paper OTC 12995.

Piper, D.J.W., and DeWolfe, M. 2002. Quaternary International, accepted.

Piper, D.J.W., and Normark, W.R. 1989. Late Cenozoic sea-level changes and the onset of glaciation: impact on continental slope progradation off eastern Canada. Marine and Petroleum Geology, 6: 336-347.

Piper, D.J.W. and Normark, W.R, 1982, Effects of the 1929 Grand Banks earthquake on the continental slope off eastern Canada. Geological Survey of Canada Paper 82-1B, 147-151.

Piper, D.J.W., and Pereira, C.P.G. 1992. Late Quaternary sedimentation in central Flemish Pass. Canadian Journal of Earth Sciences, 29: 535-550.

Piper, D.J.W. and Skene, K.I., 1998, Latest Pleistocene ice-rafting events on the Scotian Margin (eastern Canada) and their relationship to Heinrich events: Paleoceanography, v. 13, p. 205-214.

Piper, D.J.W., and Sparkes, R. 1986. Shallow sediment instability in the central part of Flemish Pass, east of the Grand Banks of Newfoundland. Geological Survey of Canada, Open File 1368.

Piper, D.J.W., Hiscott, R.N., and Normark, W.R. 1999. Outcrop-scale acoustic facies analysis and latest Quaternary development of Hueneme and Dune submarine fans, offshore California. Sedimentology, 46: 47-78.

Piper, D.J.W. and Toews, M., 2002, Late Quaternary failures at Orphan Knoll: Geological Survey of Canada Current Research 2002-E17, 8p.

Rashid, H., Hesse, R. and Piper, D.J.W. 2002, Distribution, thickness and origin of Heinrich layer 3: Earth and Planetary Science Letters (revised version returned to journal, acceptance anticipated)

Thurber Consultants Ltd. 1985, Study of well logs from East Coast offshore wells to delineate gas hydrate occurrence: Report to Earth Physics Branch, EMR, 28 p.

X. Appendix:

Figure Captions:

Fig 1a. Map of study area showing regional bathymetry, exploration lease blocks, and exploratory wells.

Fig 1b. Bathymetric map of Flemish Pass showing cores (grey dots), high resolution seismic tracks (black lines). The location of figures containing seismic reflection profiles are labelled with the figure reference and a bold black line. Cores discussed in text and illustrated in figures are labelled.

Fig 2. Three seismic-reflection profiles illustrating the Late Pliocene/Quaternary seismic stratigraphy discussed in table 2. (A) Industry multichannel seismic profile across the western margin and floor of central Flemish Pass. (B) Single channel GSCA airgun profile on the floor of Flemish Pass near the eastern side of (A). (C) Equivalent Huntec DTS profile.

Fig. 3. Seismic-reflection profile through the debris-flow deposits near the Gabriel C-60 well. Debris-flow deposits (a) to (f) are discussed in text. Shows correlation to debris-flow deposits illustrated in Figures and 8.

Fig. 4. Seismic-reflection profile showing stacked failure deposits in southern Flemish Pass.

Fig. 5. Seismic-reflection profile through Sackville Spur showing buried failure scarps and debris-flow deposits (grey overlay). Reflector violet is described in Table 2. Position of core MD2026 (Fig. 15) is projected onto the profile.

Fig. 6. Seismic-reflection profile and line drawing interpretation of debris-flow deposits in Southeastern Flemish Pass near Beothuk Knoll.

Fig. 7. Seismic-reflection profile upslope from the Gabriel Lobe showing the cut-and-fill seismic character of the western margin of Flemish Pass. Modified from Armstrong et al. (1988).

Fig. 8. Seismic-reflection profile illustrating lens-shaped amorphous zones interpreted as mass transport deposits. The inset is a Huntec DTS profile showing the geometry of near-seabed sediment waves.

Fig. 9. Schematic cross section along the length of Flemish Pass showing correlation of acoustically amorphous zones interpreted as debris-flow deposits. Location of transect is shown in Figure 1b.

Fig. 10. Type examples of Huntec DTS acoustic facies mapped throughout Flemish Pass. The results of the mapping experiment are shown in Figure 11.

Fig. 11. Results of Huntec DTS acoustic facies mapping experiment. For an explanation of acoustic facies types, see text and Figure 10.

Fig. 12. Representative piston cores from Flemish Pass, showing principal lithologies and chronostratigraphic markers including Heinrich events and radiocarbon dates (Table 1). For location of cores, see Figure 1b.

Fig. 13. Detailed graphical logs of 6 cores which form an east-west transect across the floor of central Flemish Pass.

Fig. 14. Downcore plots of the L* component (black to white) of the L*a*b* colour model showing the correlation of lighter colour L* values to Heinrich layers.

Fig. 15. Log of core MD95-2026 on Sackville Spur.

Fig. 16. Atterberg limits data for cores analysed since the report of Marsters (1991).

Fig. 17. Late Pleistocene sedimentation rates based on cores containing an undisturbed section from the floor of Flemish Pass.

Fig 18. Map illustrating the distribution of major seabed and near-seabed geological features in Flemish Pass.

Fig. 19. Tie of core 96018-12 (cf. Fig. 12) on the southern floor of Flemish Pass to seismic stratigraphy in Huntec DTS sparker profile.

Fig. 20. Tie of core 85044-003 (cf. Fig. 7) on the southwestern flank of Flemish Pass to seismic stratigraphy in Huntec DTS boomer profile.

Fig. 21. Huntec DTS sparker profile at the margin of the lobe of debris-flow deposits near the Gabriel C-60 well. (a) to (c) are debris-flow deposits also shown in Figures 3 and 22.

Fig. 22. Chronologic relationship of seismic markers, sediment facies and failure events to the global isotopic curve (McIntyre et al. 1989).

Fig. 23. Huntec DTS sparker profile on floor of the Pass showing seismic stratigraphy and acoustic facies. Inset shows acoustic character interpreted as thick sand beds. I - IV are acoustic facies described in text.

Fig. 24. Tie of core MD95-2026 (cf Fig. 15) on Sackville Spur to seismic stratigraphy in Huntec DTS profile. Large diapirs (pagoda structures, Emery, 1984) are present on the left of the profile.

Tables:

Table 1- Radiocarbon dating information for cores from Flemish Pass.

Core	depth (cm)	material	Age*	Lab no.
Previously unreported dates:				
87008-013TWC	80	foraminifera	11900 + 110	TO-4487
87008-013TWC	125	shell fragments	11810 + 90	TO-5210
87008-013	597	scaphopod	13120 + 100	TO-7924
87008-013	920	bivalve shell fragments	23130 +190	TO-7925
MD95-2026	632	Clam shell fragments	52570 + 2220	TO-6356
96018-003	84	scaphopod fragments	13520 +160	TO-6663
96018-003	458	mollusc fragments	42630 + 720	TO-6197
96018-005TW	42	scaphopod	13240 + 90	TO-6198
96018-005	79	mollusc fragments	16620 + 110	TO-6199
96018-005	472	bivalve	36650 + 470	TO-6200
96018-006	576	bivalve fragments	27980 + 240	TO-7923
96018-006	652	bivalve fragments	33240 + 500	Beta 149803
96018-007	303	scaphopod	14870 + 140	TO-6543
96018-008	108	scaphopod	13250 + 90	TO-6464
96018-008	172	gastropod	14550 + 100	TO-6465
96018-008	335	mollusc fragments	21280 + 170	TO-6467
96018-008	193	mollusc fragments	35570 + 400	TO-6466
86018-012	42	mollusc fragments	14770 + 170	TO-5968
99031-004	235	foraminifera	27190 + 190	Beta 167347
99031-004	388	foraminifera	>47890	Beta 167348
Piper and Pereira (1992):				
77014-009	737		27490 +120	TO-2043
85044-003	760		>33000	Beta 16483
87008-013TWC	125		11810 +90	TO-2041
87008-013	737		19200 +450	Beta 22232, ETH 3209
87008-015	645		23600 +380	Beta 22233, ETH 3210
87008-018	34		1810 +120	Beta 22234, ETH 3211
87008-018	50		1950 +130	Beta 22235, ETH 3212
Piper and Skene (1998):				
85044-003	19	bivalve fragments	14100 + 120	TO-5967
86018-012	44	bivalve fragments	14770 + 170	TO-5968
Rashid et al. (2002):				
96018-006	159		15050 + 55	OS-33013
96018-006	508		27450 + 130	OS-33014
96018-006	576		27530 + 240	TO-7923
96018-006	660		33250 + 290	OS-33015

*Ages reported as conventional C-14 ages with no marine reservoir correction.

Table 2. Late Pliocene and Quaternary seismic stratigraphy

Reflector name	Data type (Huntec or Airgun)	Other references*	Character on W. Flemish Pass Slope	Tentative age	Basis of age estimate and other notes
Red	Huntec	Alpha[1]	local unconformity	22 ka	Heinrich layers in 85044-003 (Fig. 20). Corresponds to alpha, dated by C-14 in cores (Piper and Pereira 1992) (Fig. 10)
Orange	Huntec	Red[2], Unconf. 1[1]	top of transparent section	75 ka	C-14, isotopes in MD95-2029 (Fig. 15). Corresponds to unconformity 1 of Piper and Pereira (1992).
Yellow	Huntec	Orange[2]		130 ka	Extrapolated sedimentation rates (Fig. 8, 23)
Green	Airgun and huntec	Green (huntec)[2]		220 ka	Extrapolated sedimentation rates
Blue	Airgun	Green (airgun)[2]		350 ka	Extrapolated sedimentation rates (Fig. 3)
Violet	Airgun	Red[1]	base of section with deep slope channels	850 ka	Extrapolated sedimentation rates (Fig. 3, 5). ?corresponds to MIS 22.
Brown	Airgun	C'[3]	Deepest shallow slope channels	1.8 Ma	Speculative regional correlation by Piper and Normark (1989)
Magenta	Airgun	Blue[4]		L. Pliocene	Between brown and grey
Grey	Airgun	Purple[1], ~D'[3]		L. Pliocene	Correlated with sequence on Scotian Slope which is tied to exploratory wells

* as referred to in other papers, [1] Piper and Sparkes (1986), [2] Campbell (1997), [3] Piper and Normark (1989), [4] Armstrong et al. (1988).

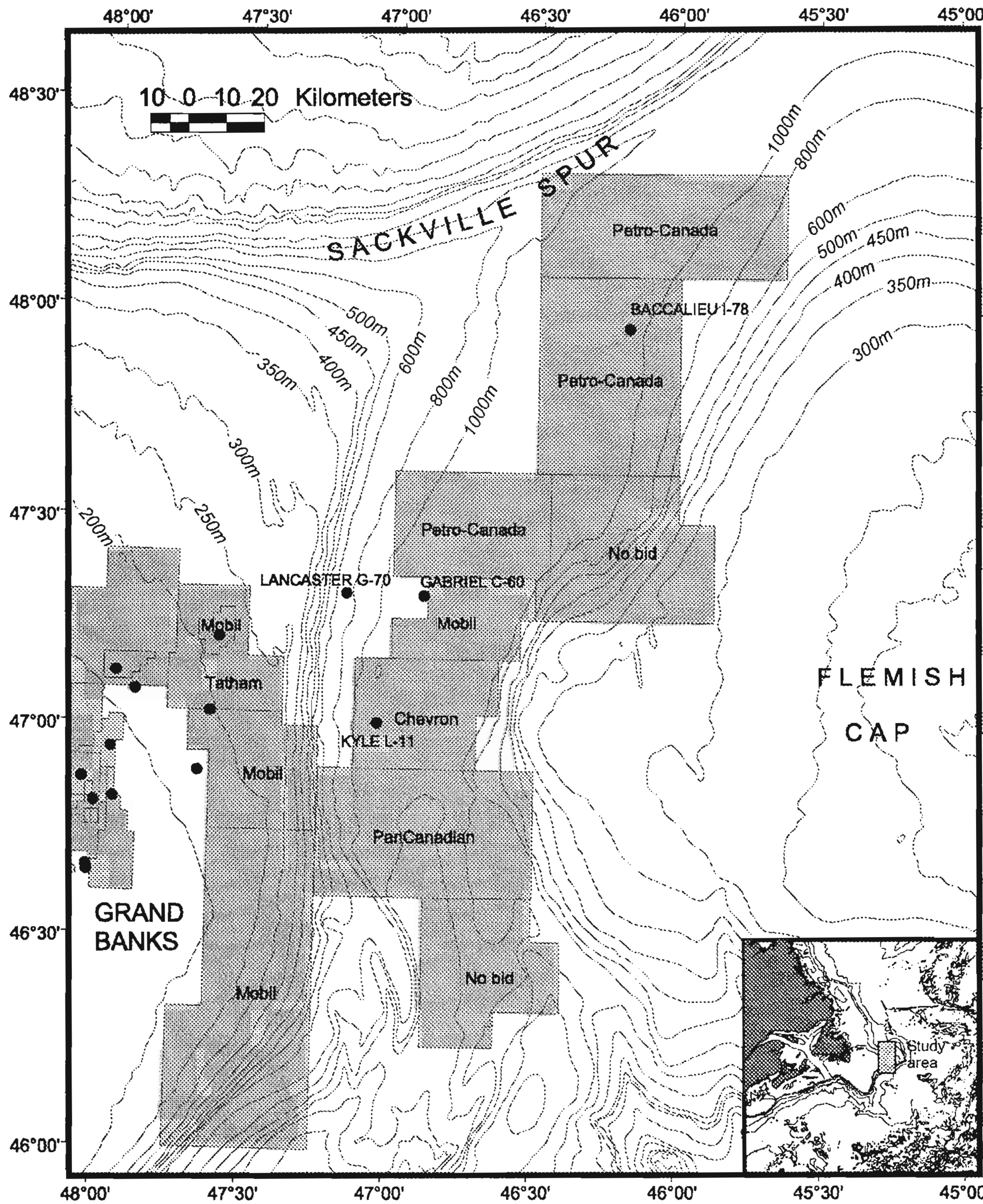

Fig 1a. Map of study area showing regional bathymetry, exploration lease blocks, and exploratory wells.

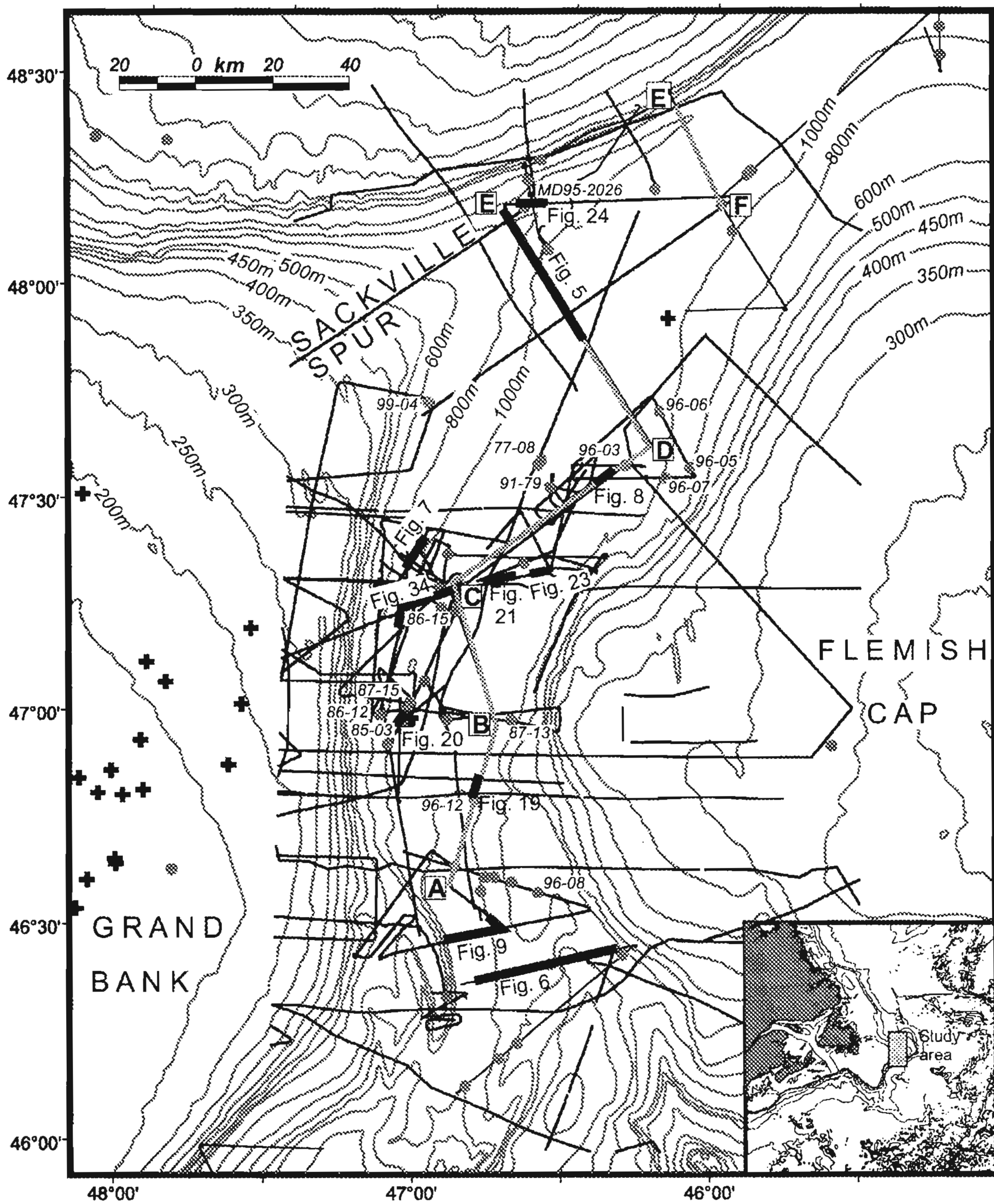

Fig 1b. Bathymetric map of Flemish Pass showing cores (grey dots), high resolution seismic tracks (black lines). The location of figures containing seismic reflection profiles are labelled with the figure reference and a bold black line. Cores discussed in text or illustrated in figures are labelled.

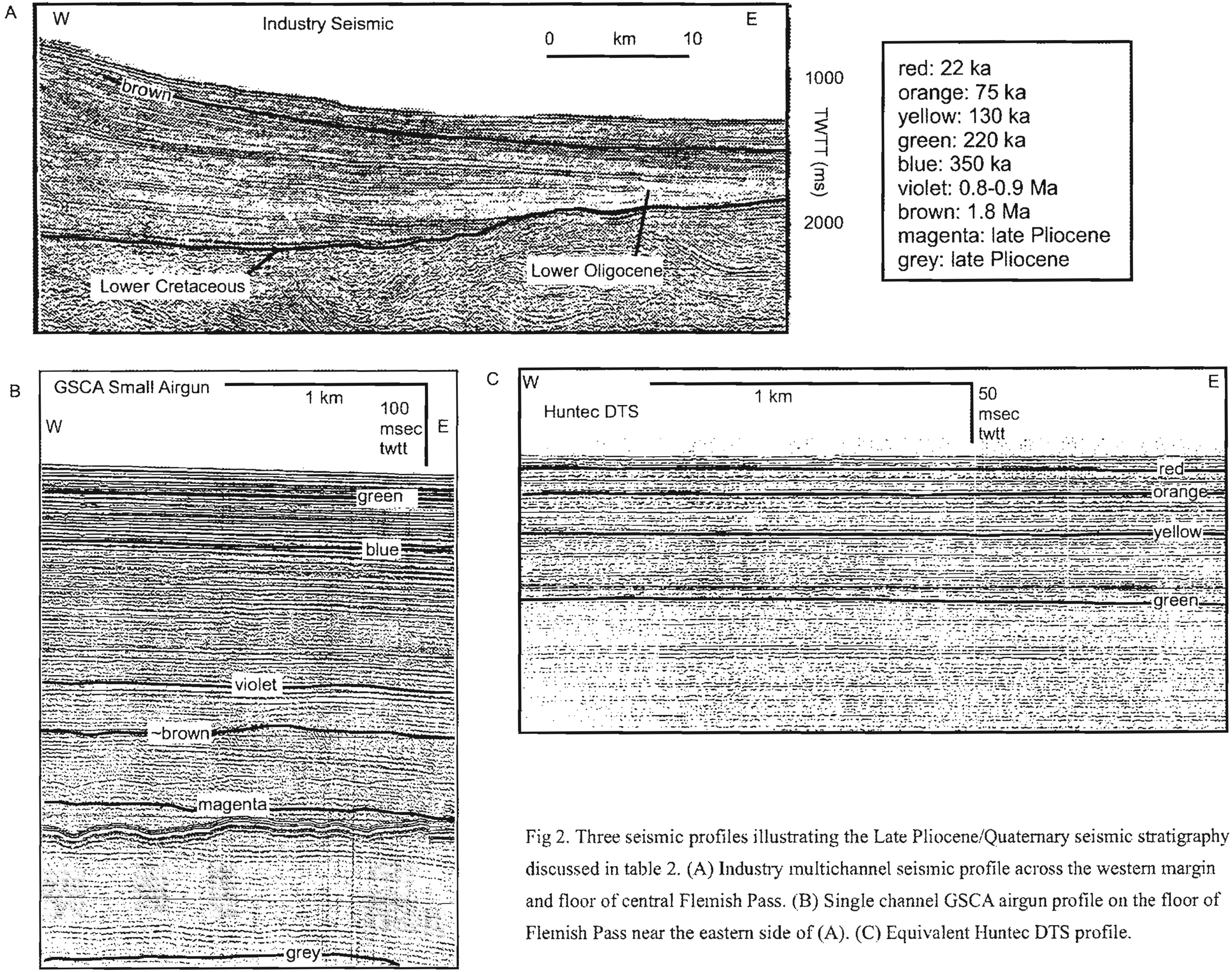

Fig 2. Three seismic profiles illustrating the Late Pliocene/Quaternary seismic stratigraphy discussed in table 2. (A) Industry multichannel seismic profile across the western margin and floor of central Flemish Pass. (B) Single channel GSCA airgun profile on the floor of Flemish Pass near the eastern side of (A). (C) Equivalent Huntec DTS profile.

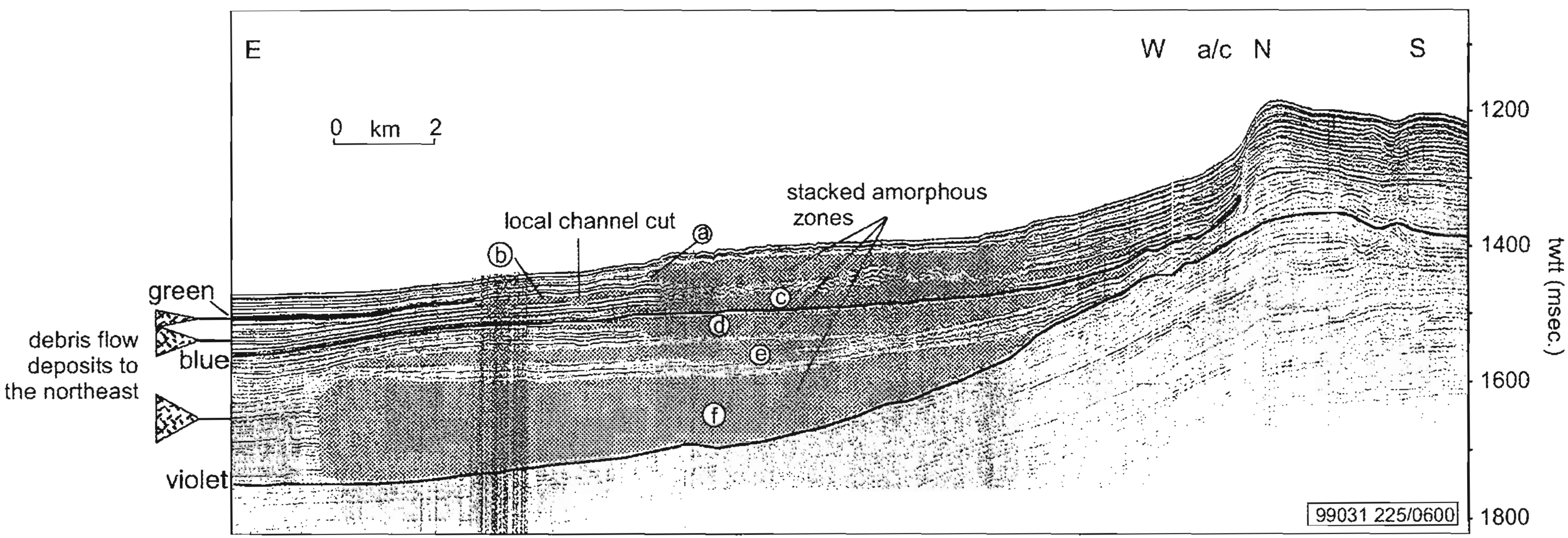

Fig. 3. Seismic-reflection profile through the debris-flow deposits near the Gabriel C-60 well. Debris-flow deposits (a) to (f) are discussed in text. Shows correlation to debris-flow deposits illustrated in Figures 5 and 8.

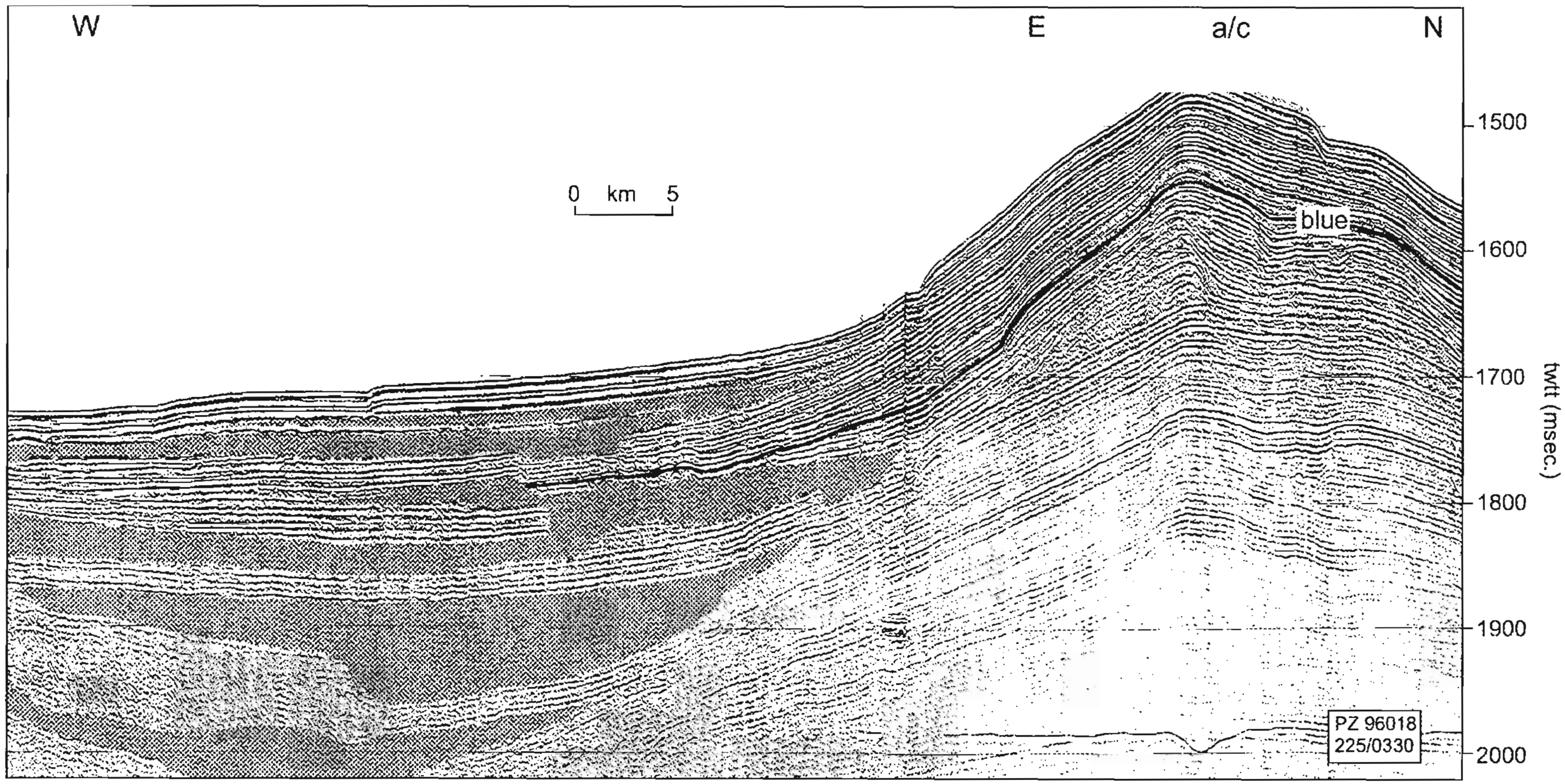

Fig. 4. Seismic-reflection profile showing stacked failure deposits in southern Flemish Pass.

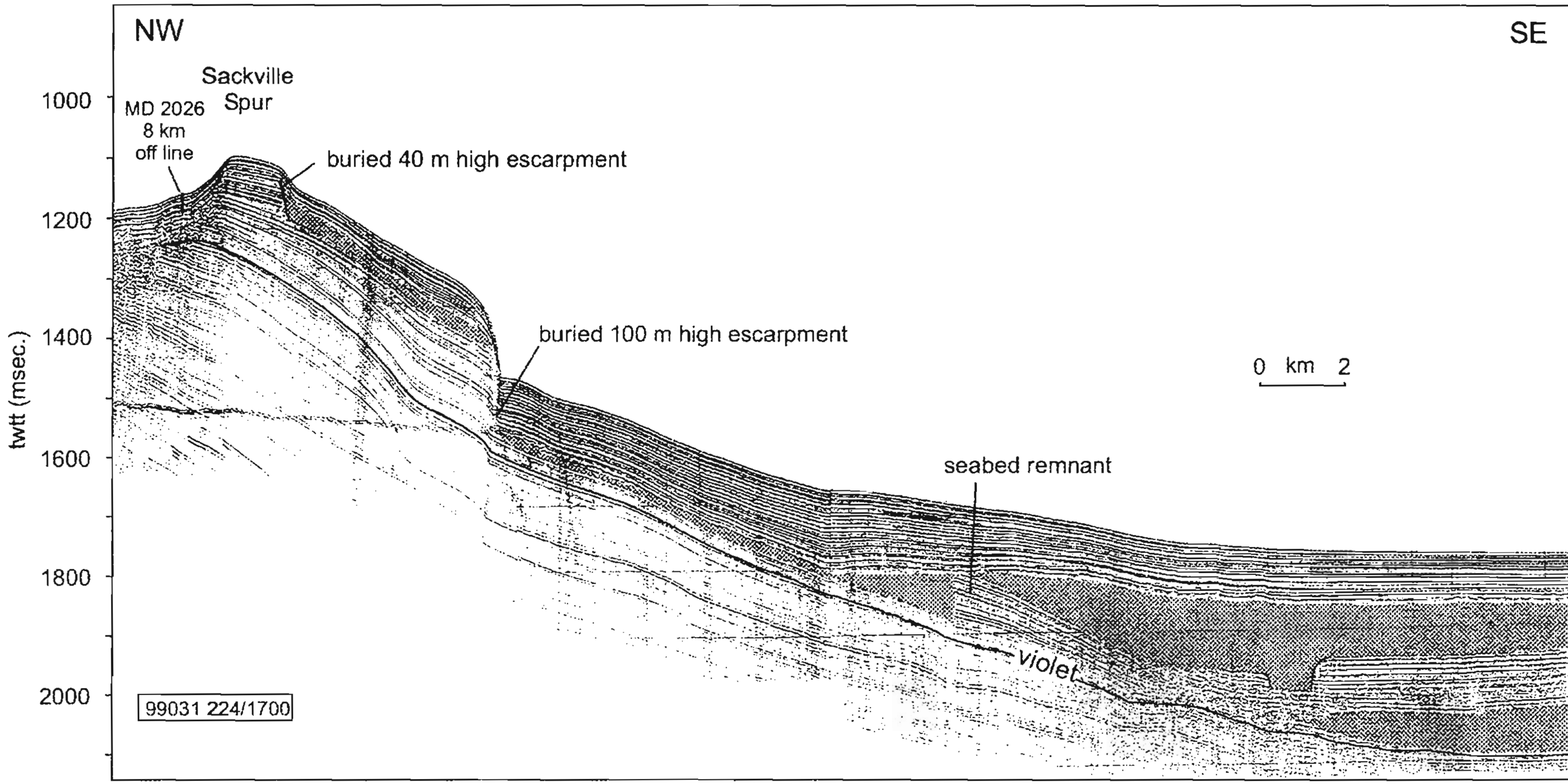

Fig. 5.Seismic-reflection profile through Sackville Spur showing buried failure scarps and debris-flow deposits (grey overlay). Reflector violet is described in Table 2. Position of core MD2026 (Fig. 15) is projected onto the profile.

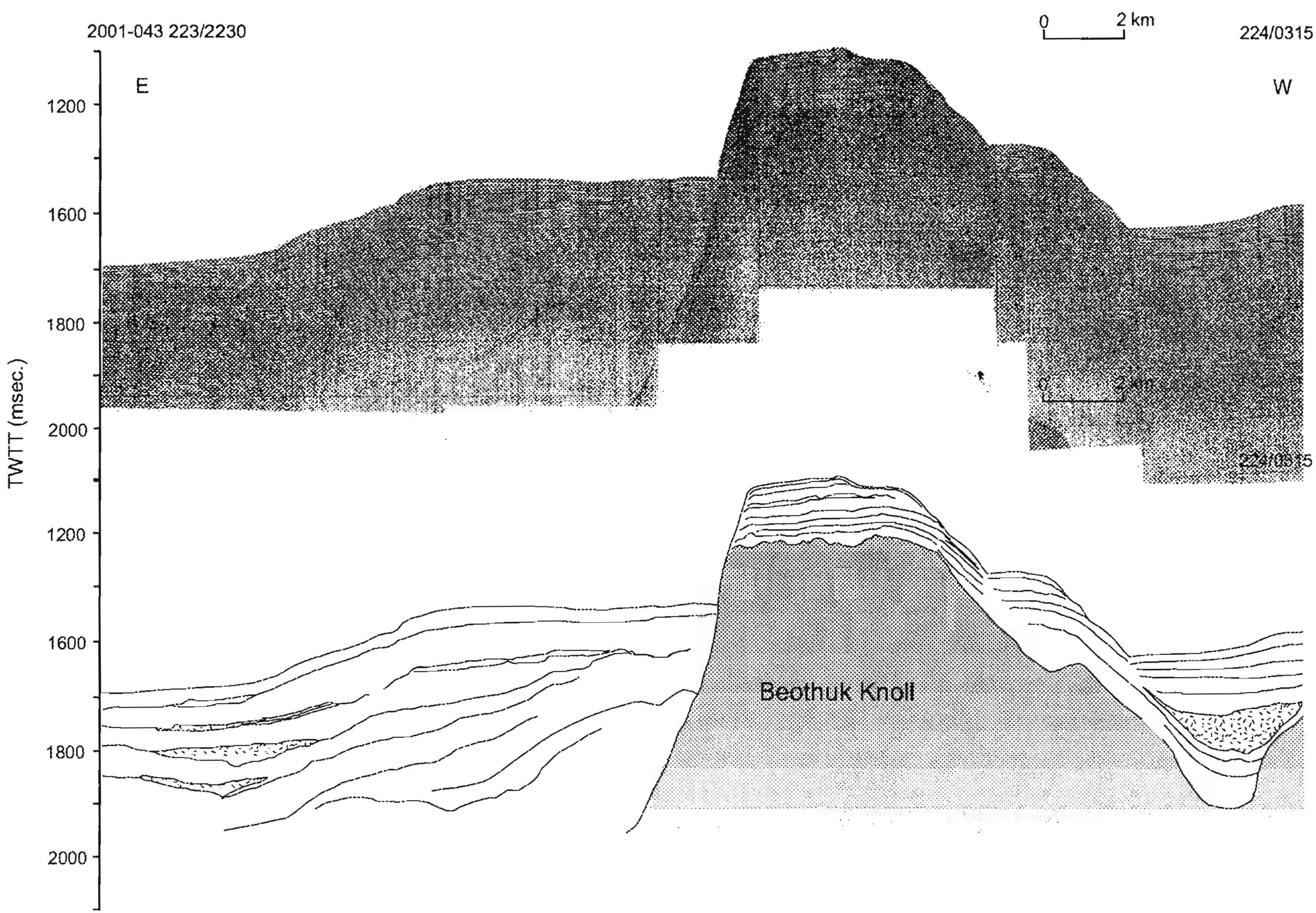

Fig. 6. Seismic-reflection profile and line drawing interpretation of debris-flow deposits in Southeastern Flemish Pass near Beothuk Knoll.

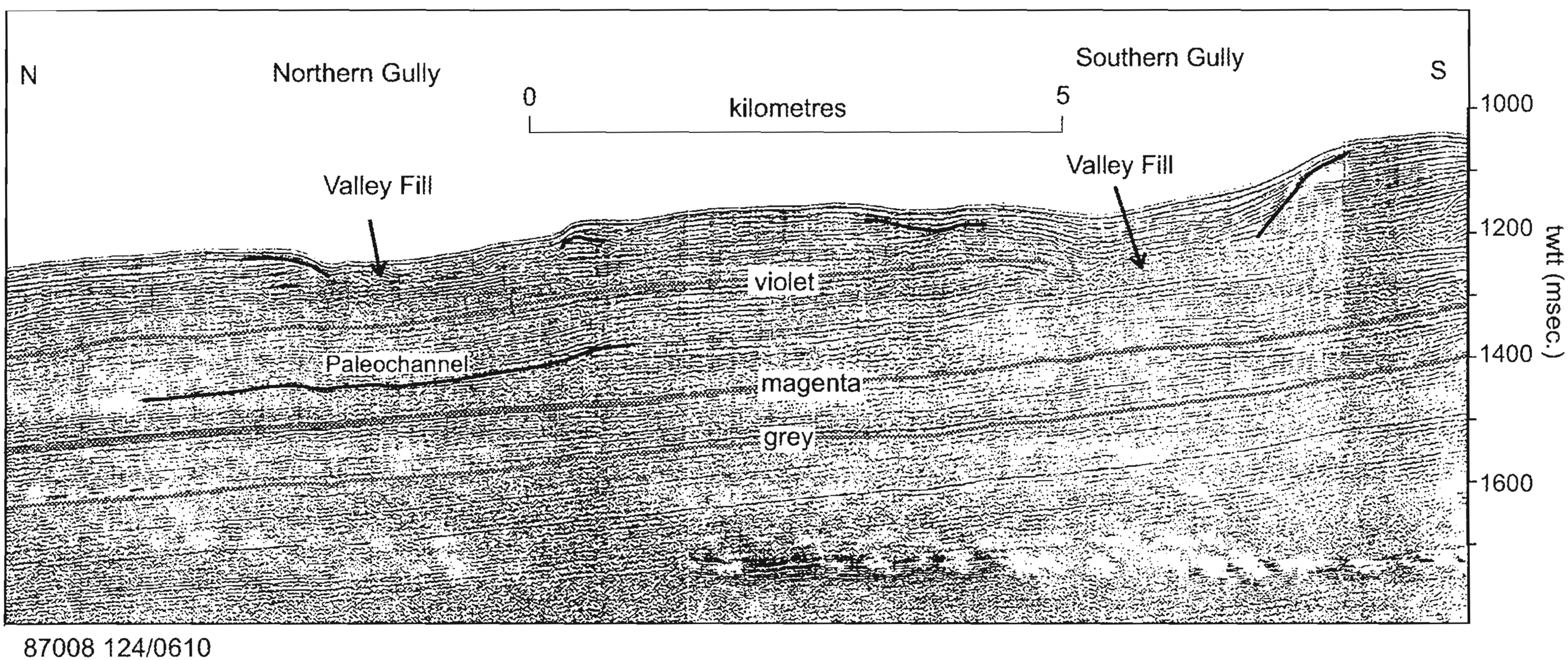

Fig. 7. Seismic-reflection profile upslope from the Gabriel Lobe showing the cut-and-fill seismic character of the western margin of Flemish Pass. Modified from Armstrong et al. (1988).

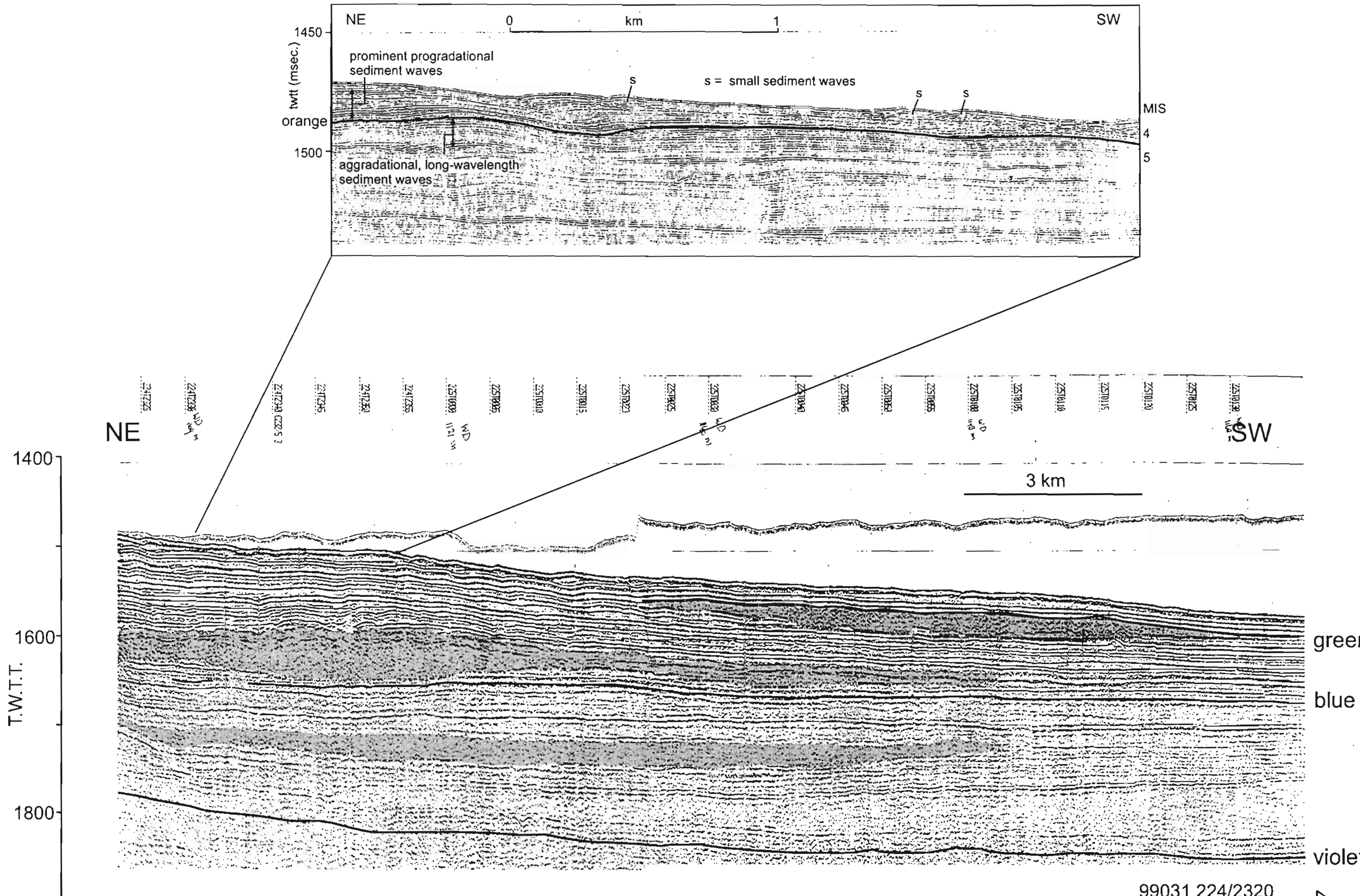

Fig. 8. Seismic-reflection profile illustrating lens-shaped amorphous zones interpreted as mass transport deposits. The inset is a Huntec DTS profile showing the geometry of near- seabed sediment waves.

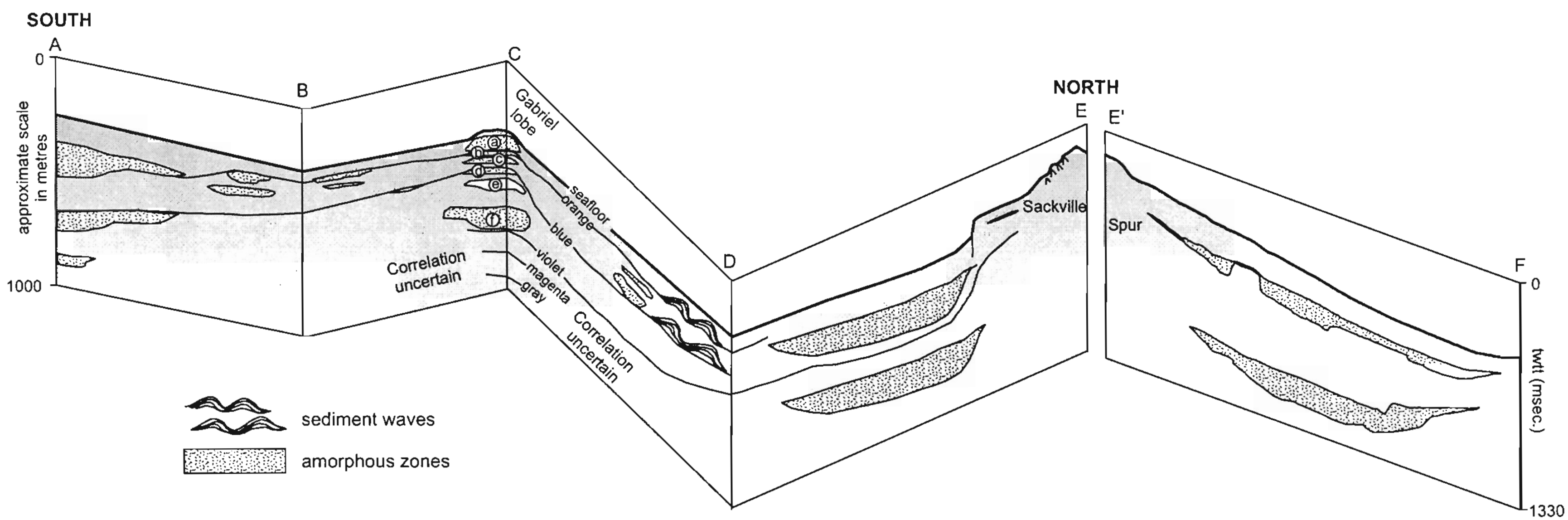

Fig. 9. Schematic cross section along the length of Flemish Pass showing correlation of acoustically amorphous zones interpreted as debris-flow deposits. Location of transect is shown in Figure 1b.

Flemish Pass Facies Type Legend

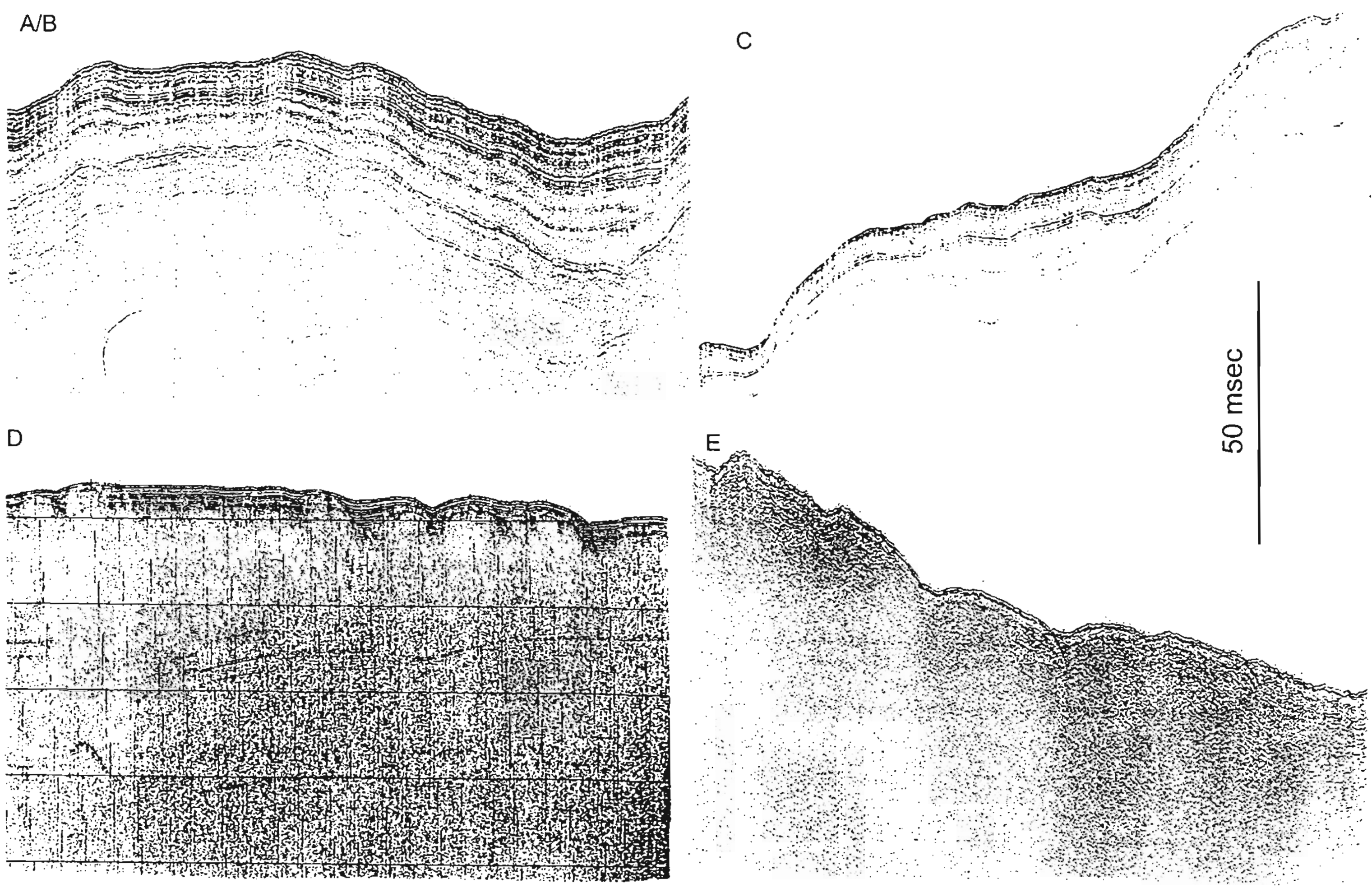

Fig. 10. Type examples of Huntec DTS acoustic facies mapped throughout Flemish Pass. The results of the mapping experiment are shown in Figure 11.

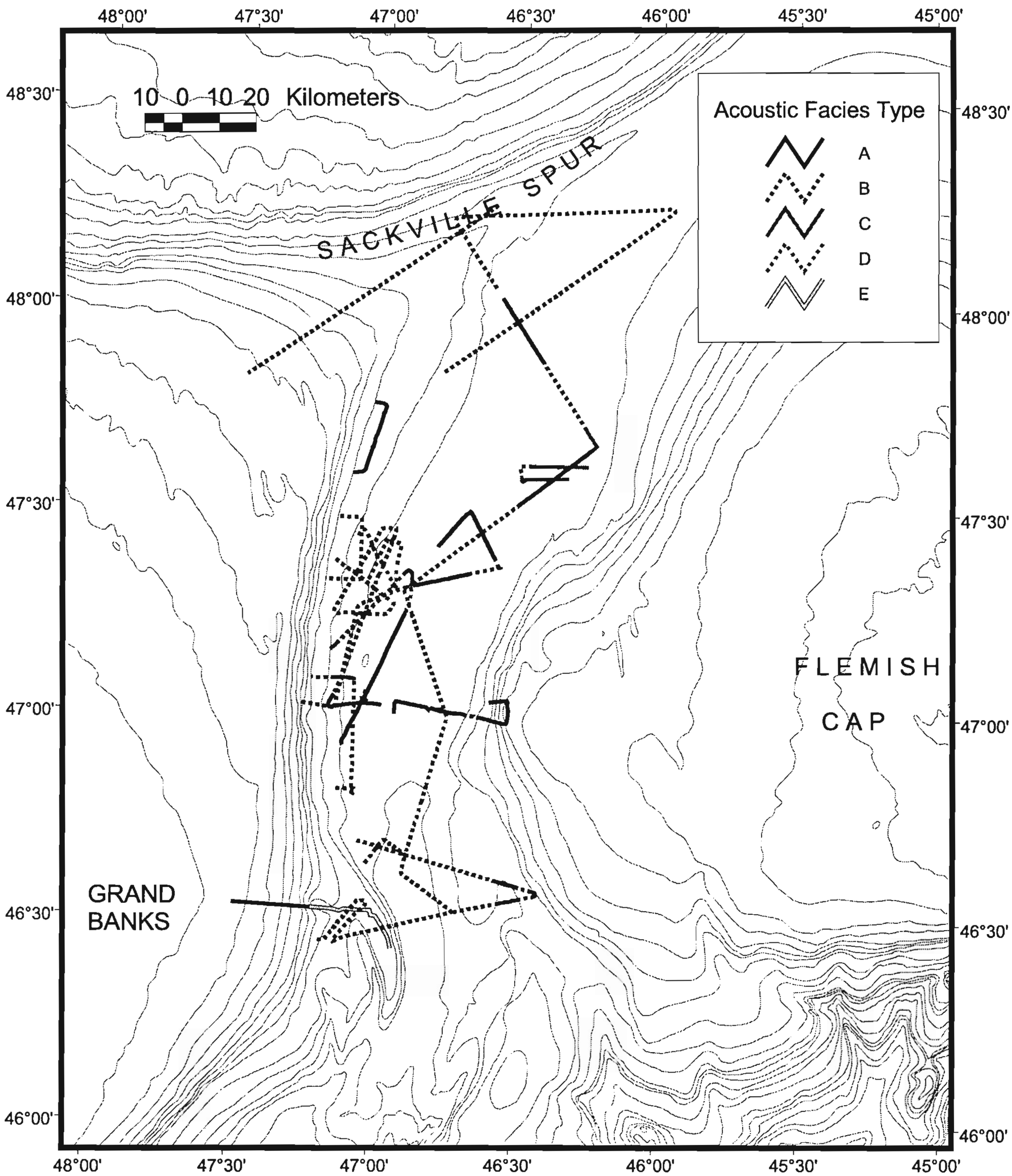

Fig. 11. Results of Huntec DTS acoustic facies mapping experiment. For an explanation of acoustic facies types, see text and Figure 10.

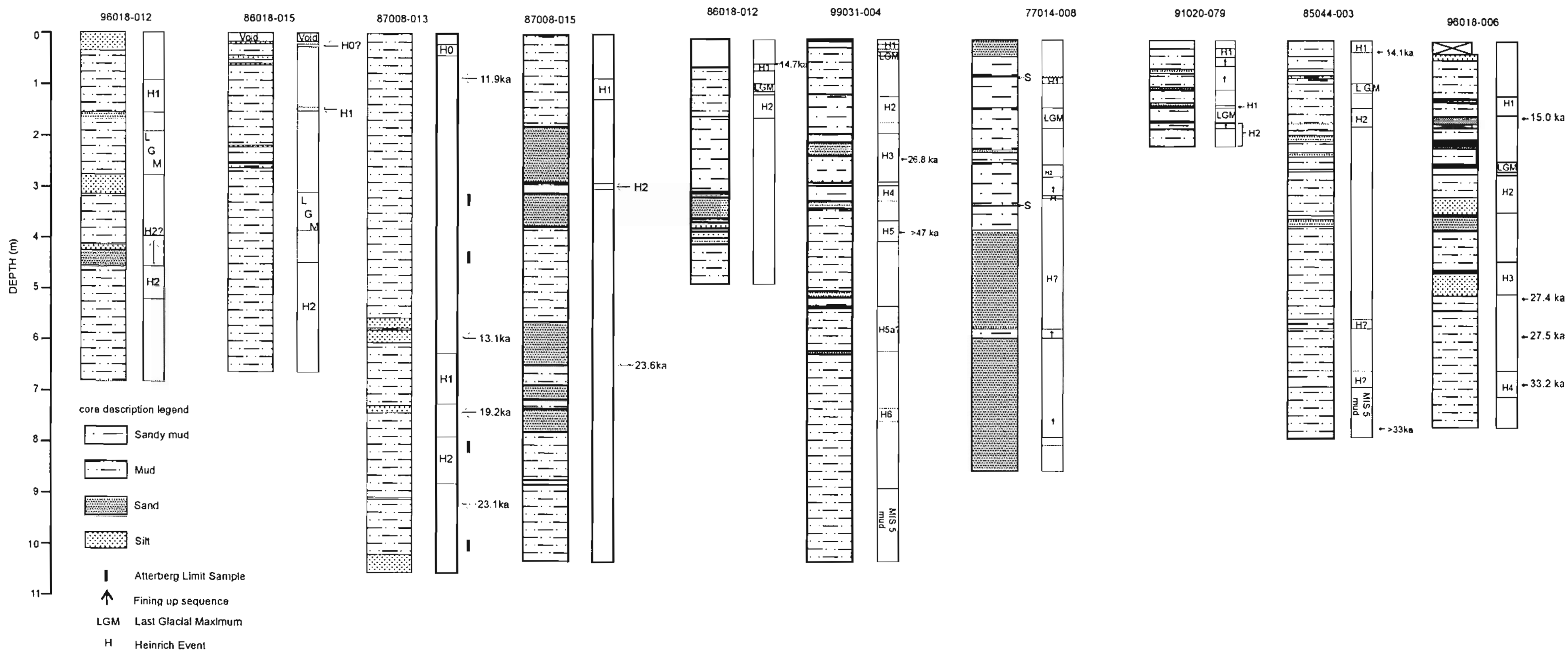

Fig. 12. Representative piston cores from Flemish Pass, showing principal lithologies and chronostratigraphic markers including Heinrich events and radiocarbon dates (Table 1). For location of cores, see Figure 1b.

50 50 90

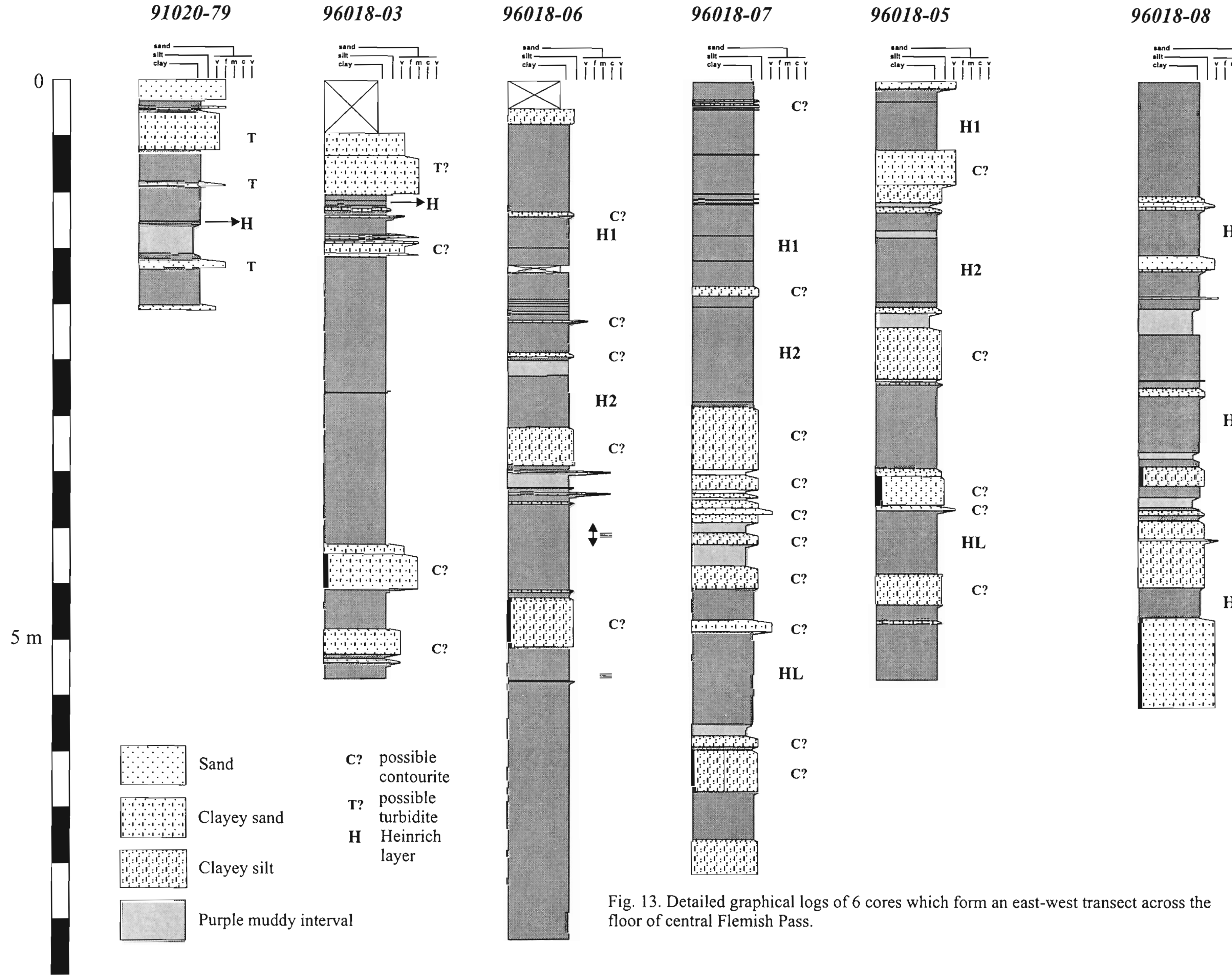

Fig. 13. Detailed graphical logs of 6 cores which form an east-west transect across the floor of central Flemish Pass.

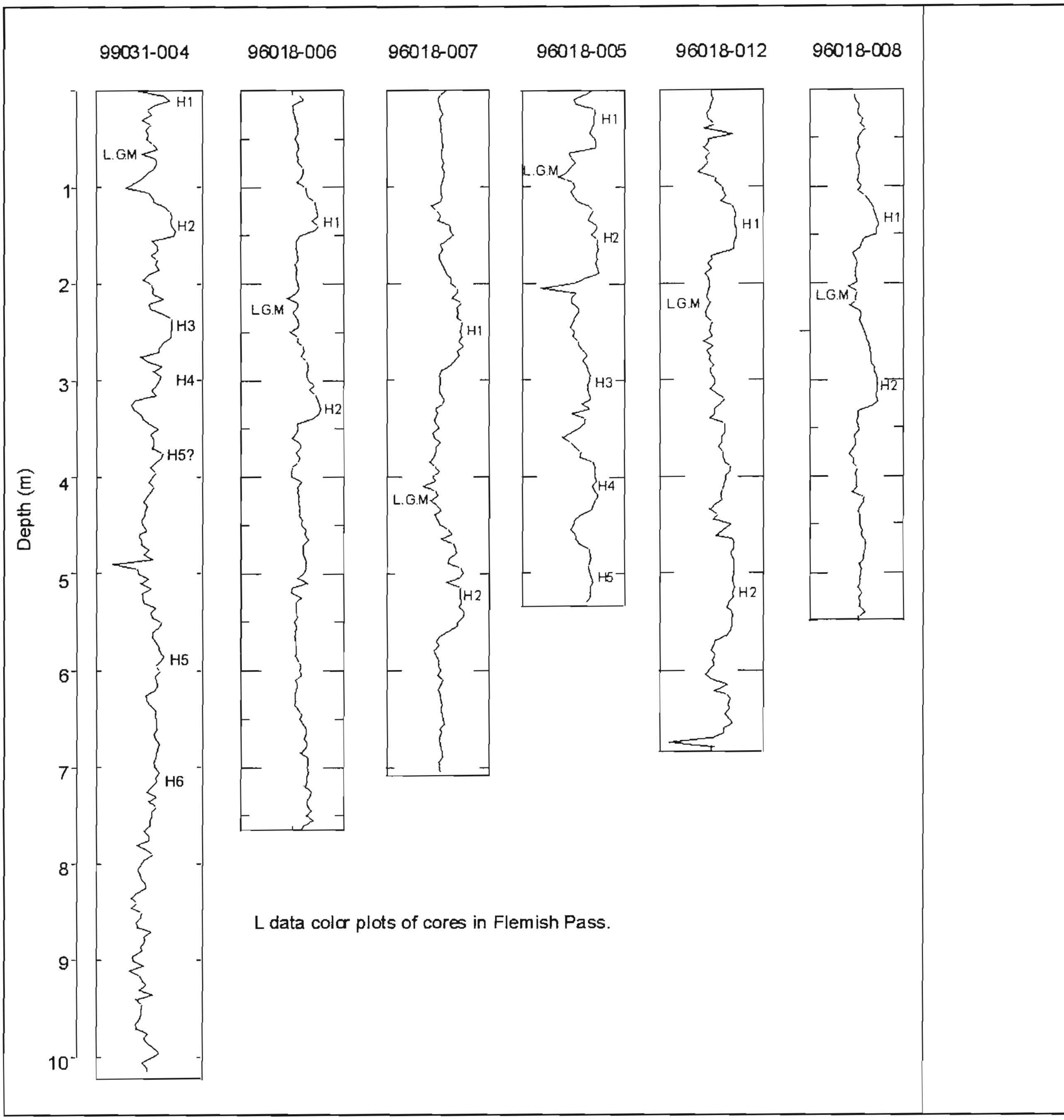

Fig. 14. Downcore plots of the L* component (black to white) of the L*a*b* colour model showing the correlation of lighter colour L* values to Heinrich layers.

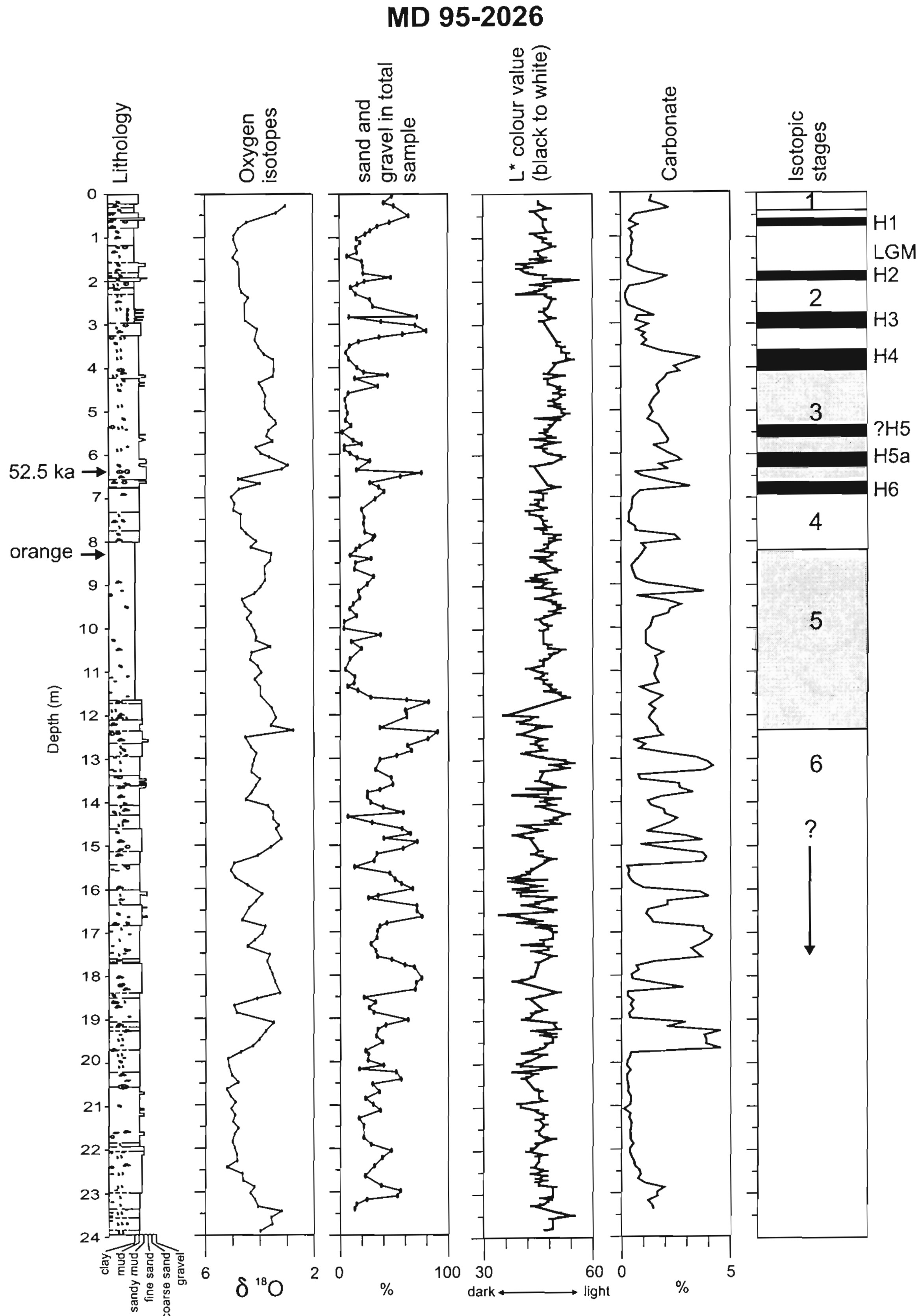

Fig. 15. Log of core MD95-2026 on Sackville Spur.

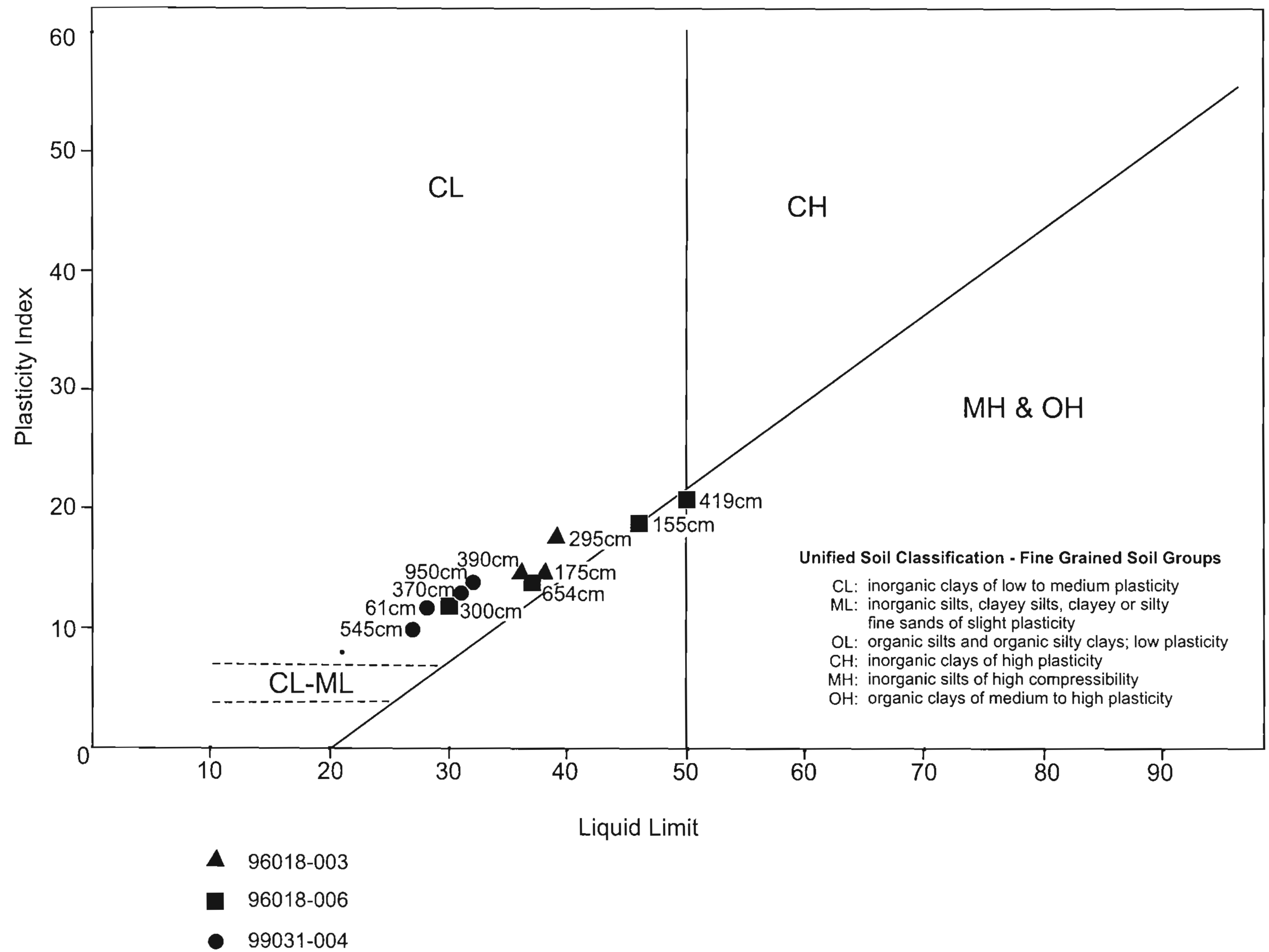

Fig. 16. Atterberg limits data for cores analysed since the report of Marsters (1991).

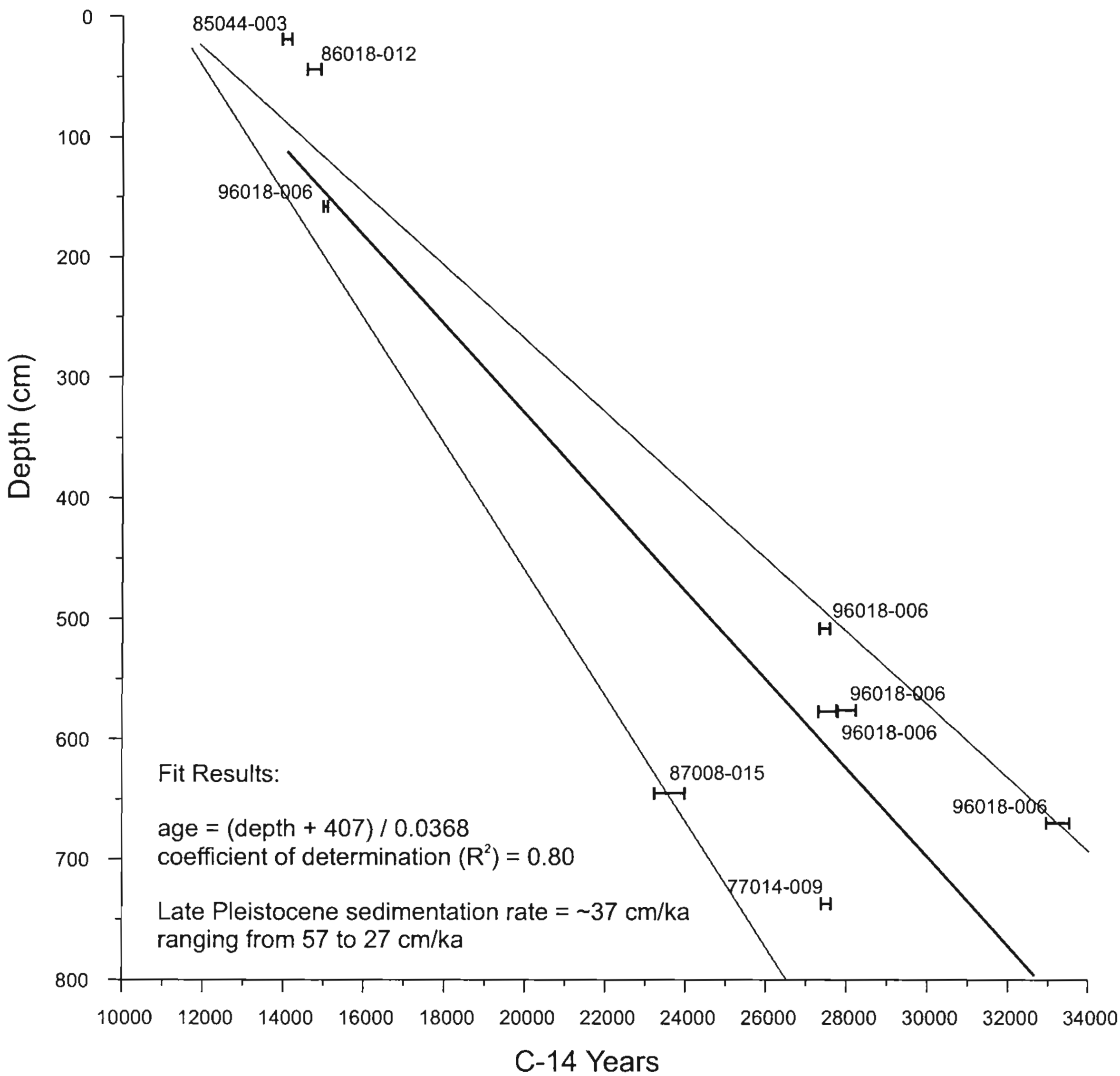

Fig. 17. Late Pleistocene sedimentation rates based on cores containing an undisturbed section from the floor of Flemish Pass.

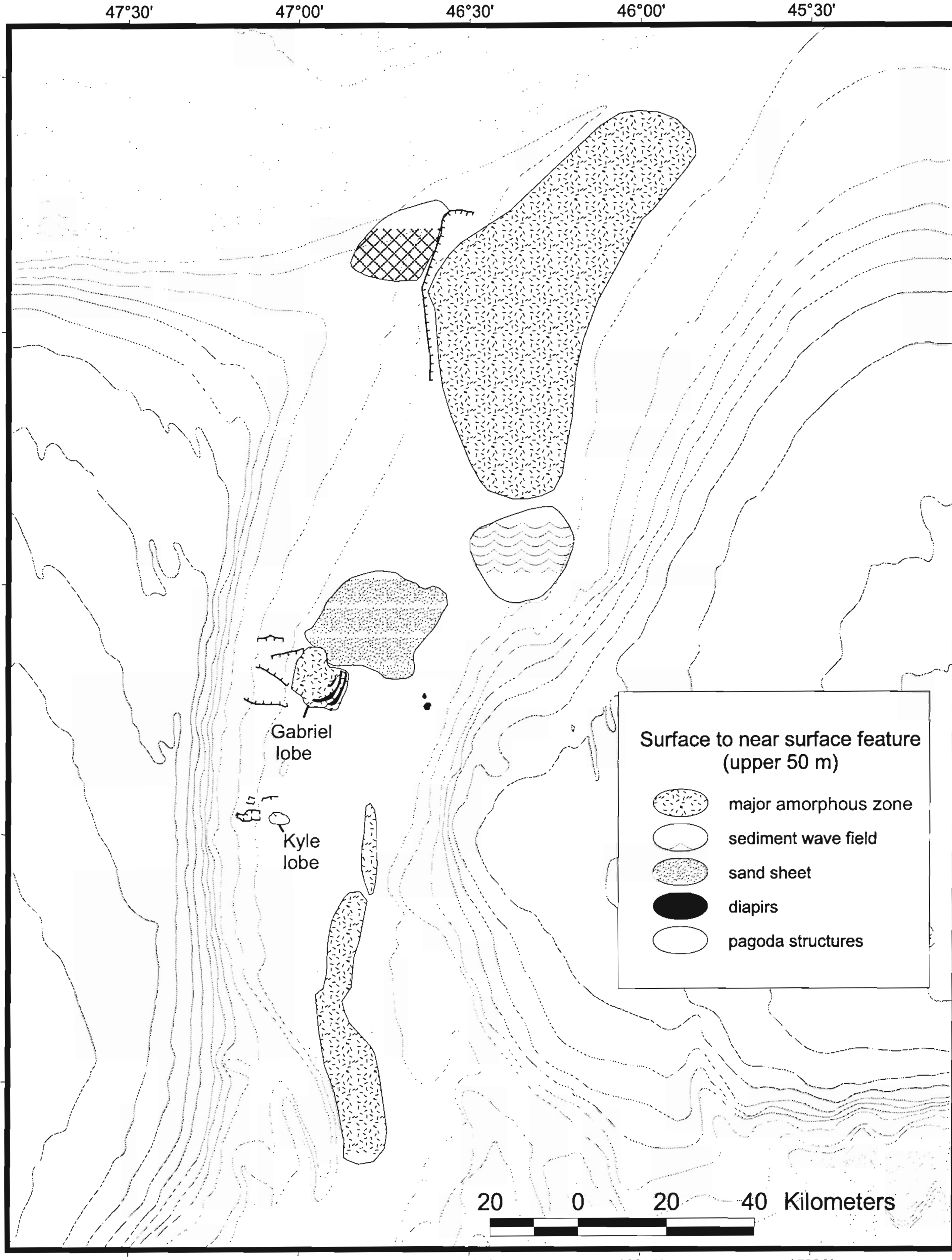

Fig 18. Map illustrating the distribution of major seabed and near-seabed geological features in Flemish Pass.

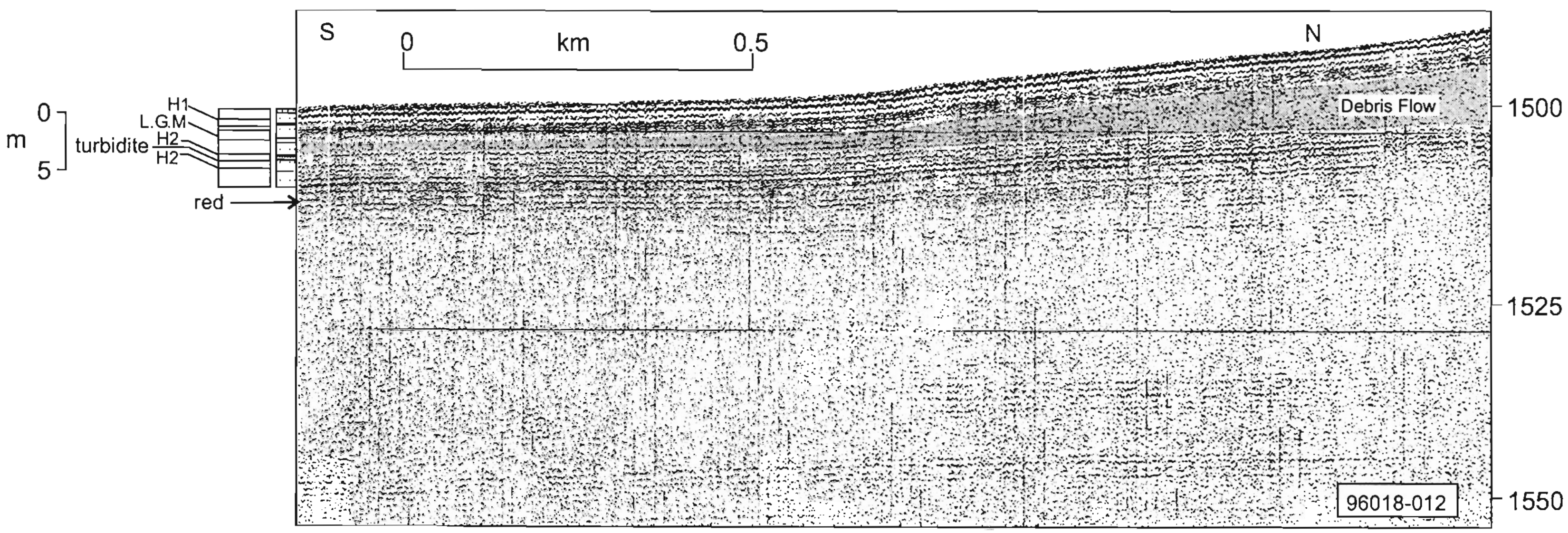

Fig. 19. Tie of core 96018-12 (cf. Fig. 12) on the southern floor of Flemish Pass to seismic stratigraphy in Huntec DTS sparker profile.

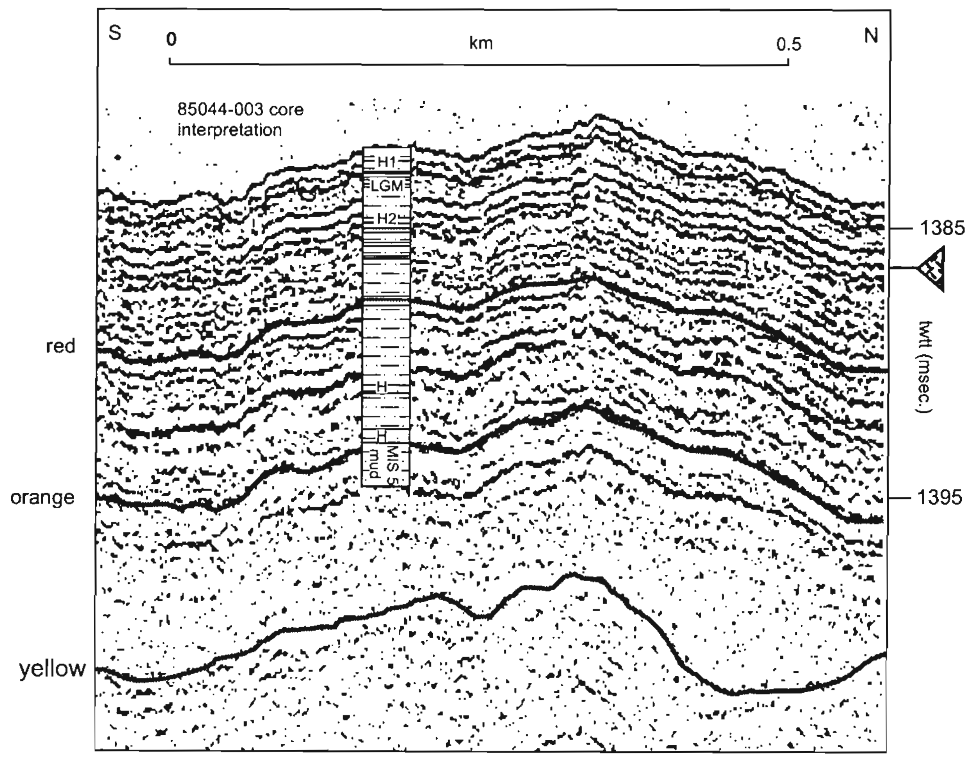

Fig. 20. Tie of core 85044-003 (cf. Fig. 7) on the southwestern flank of Flemish Pass to seismic stratigraphy in Huntec DTS boomer profile.

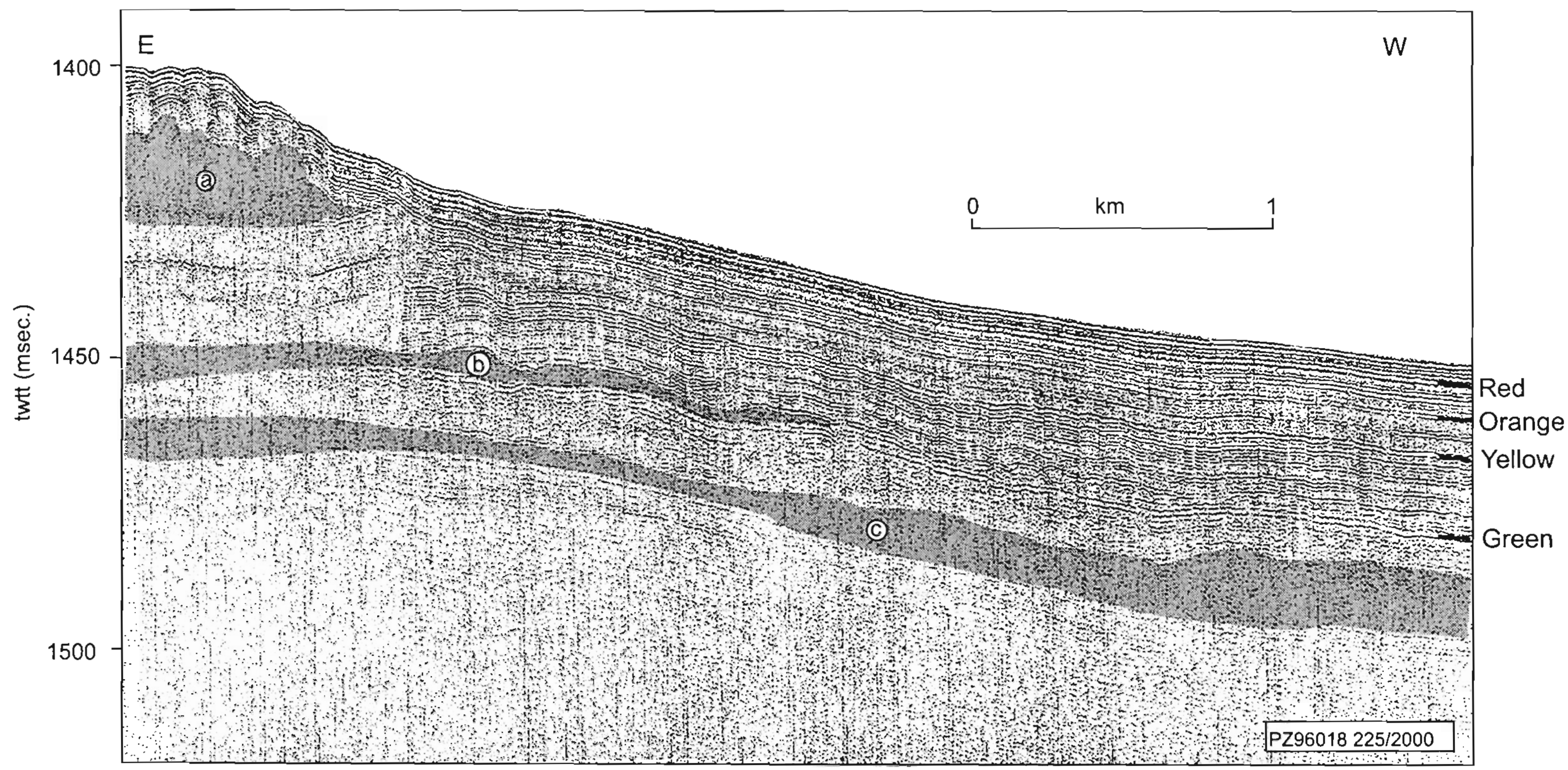

Fig. 21. Huntec DTS sparker profile at the margin of the lobe of debris-flow deposits near the Gabriel C-60 well. (a) to (c) are debris-flow deposits also shown in Figures 3 and 22.

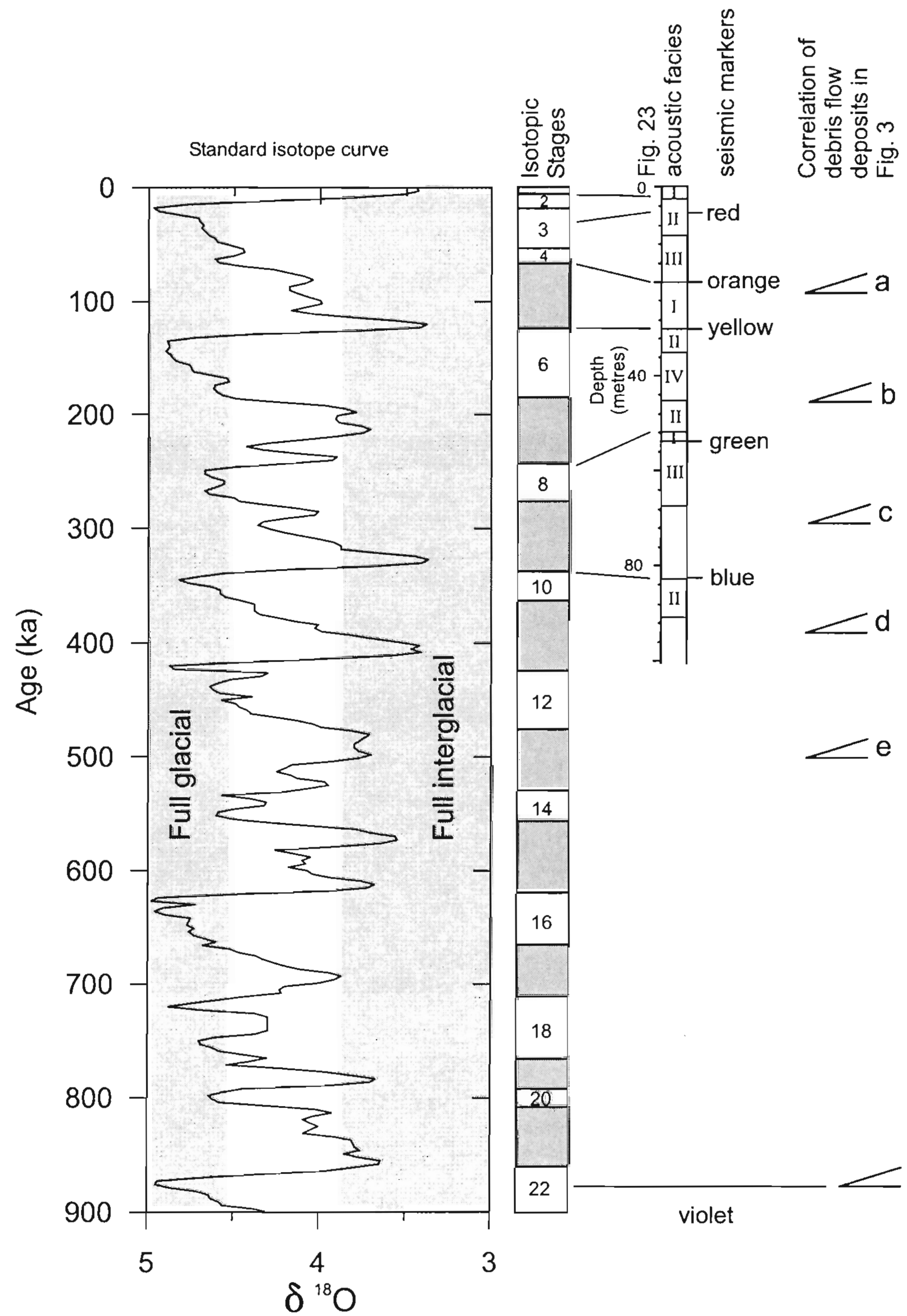

Fig. 22. Chronologic relationship of seismic markers, sediment facies and failure events to the global isotopic curve (McIntyre et al. 1989).

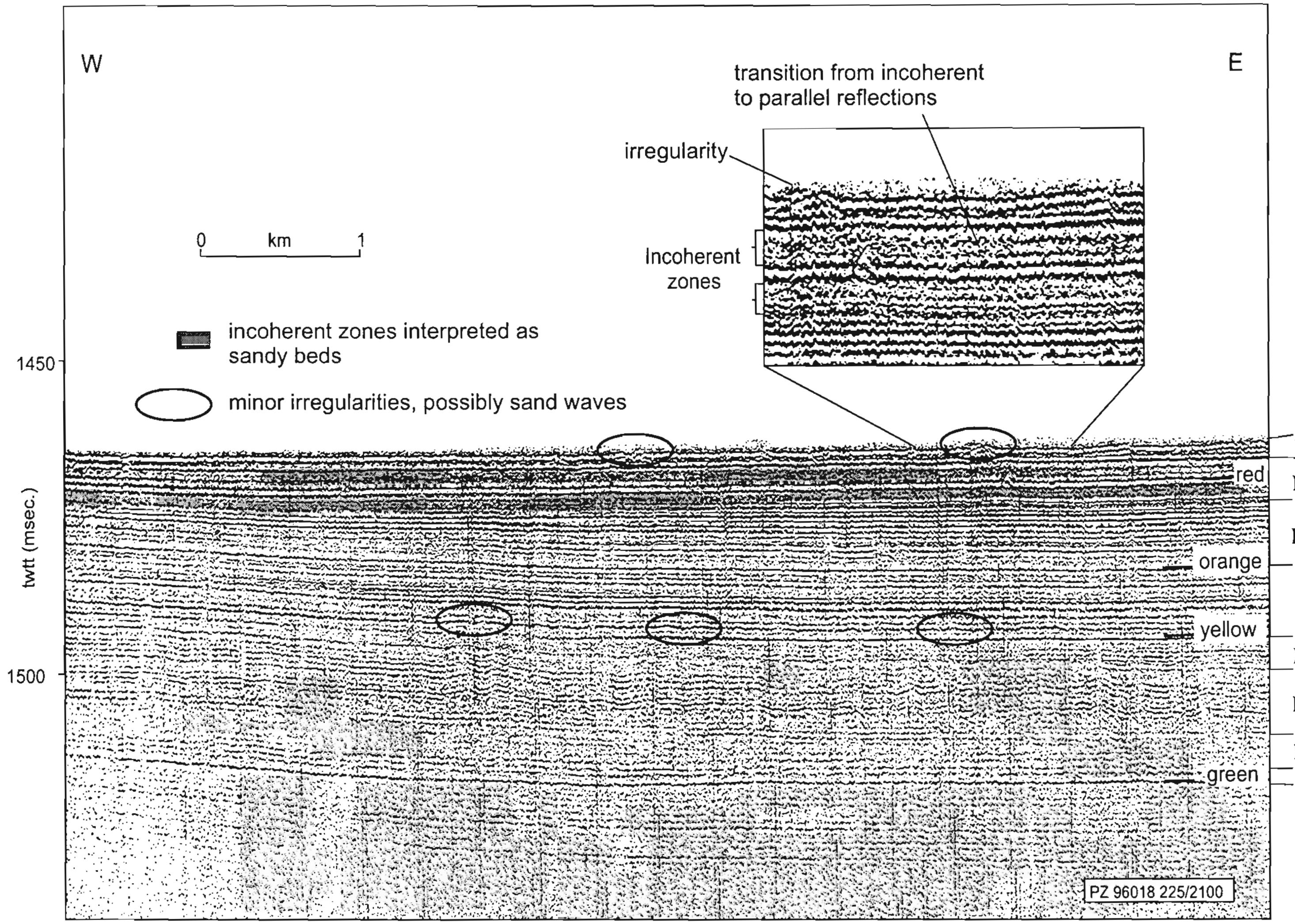

Fig. 23. Huntec DTS sparker profile on floor of the Pass showing seismic stratigraphy and acoustic facies. Inset shows acoustic character interpreted as thick sand beds. I - IV are acoustic facies described in text.

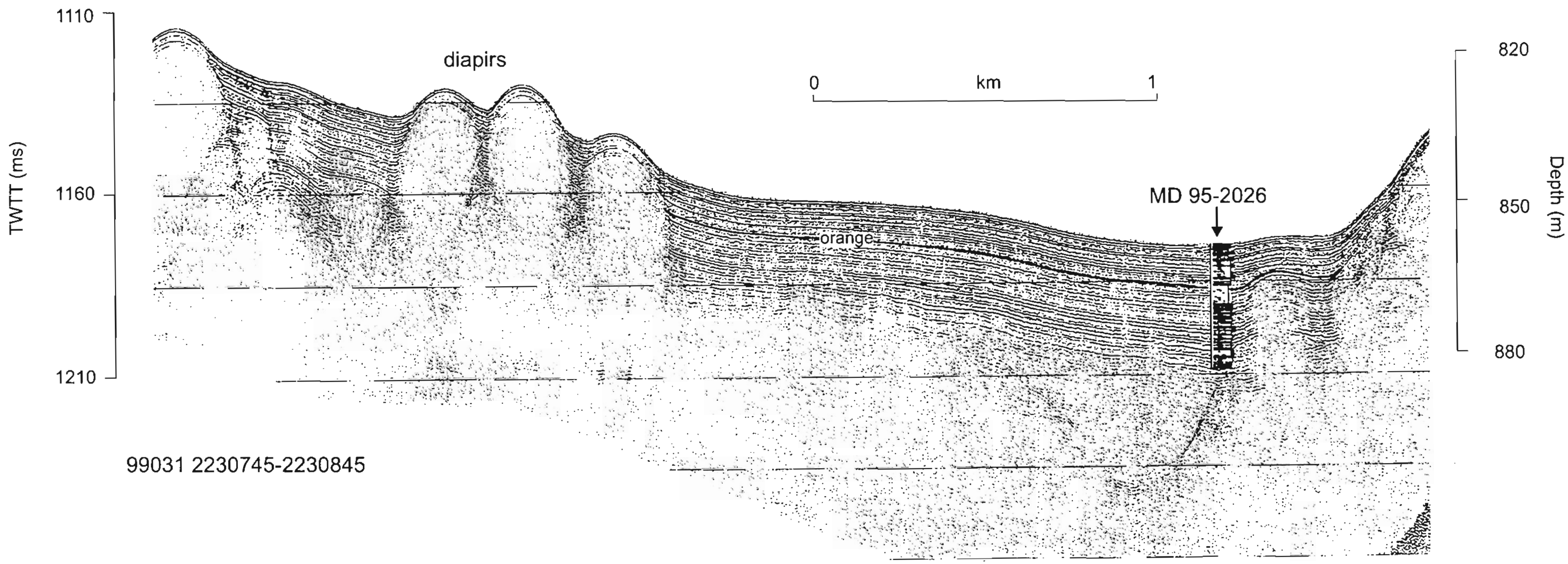

Fig. 24. Tie of core MD95-2026 (cf Fig. 15) on Sackville Spur to seismic stratigraphy in Huntec DTS profile. Large diapirs (pagoda structures, Emery, 1984) are present on the left of the profile.